Evaluating Mitochondrial Transport in CHCHD10 S59L-Mediated ALS-FTD

A Thesis
SUBMITTED TO THE FACULTY OF THE
UNIVERSITY OF MINNESOTA
BY

Madeleine Rose Chalmers

IN PARTIAL FULFILLMENT OF THE REQUIREMENTS
FOR THE DEGREE OF
MASTER OF SCIENCE

Nam Chul Kim, Advisor

August 2024

Acknowledgements

First, I would like to thank my advisor, Dr. Kim, for taking me in as an undergraduate and letting me stay for the last 6 years, and for fueling my curiosity with this study. You challenged me and helped me learn what it means to be a scientist. I would also like to thank my committee members, Dr. Amy Yang, Dr. Tommy Bastian, and Dr. Sarah Lacher for their support and expertise along the way. I especially want to thank Sarah for being a sound board and keeping me sane during the past 3 years.

Second, I'd like to thank Kayla Johnson for kicking my butt as a spin instructor, and for being my expert in SH-SY5Y differentiation. The 2 pages of my thesis dedicated to SH-SY5Y cell culture and differentiation does not do our 1 year of troubleshooting justice. I wouldn't have gotten as far as I did without you.

Third, I'd like to thank the countless people in the IBS program for the endless cribbage games, nerd conversations, and laughs. I'd also like to thank Stormi Davis-Hagadone, Dr. Jennifer Liang, and Dr. Sara Zimmer for being my advocates over the last 3 years.

Finally, I'd like to thank my family and friends for their unwavering support and encouragement. A special shoutout to the women in book club, especially Amy Bowman, for helping me find my love for reading again. I always looked forward to our monthly meetings. A very, very special thank you goes to my partner, Jeremiah, who has been my absolute rock during graduate school. I am truly blessed to have you in my life.

Abstract

Amyotrophic lateral sclerosis with frontotemporal dementia (ALS-FTD) is a lethal age-progressive disease characterized by motor and behavioral deficits, as well as personality changes. With no effective treatments and its complex clinical spectrum, there is a great need to further elucidate the pathogenesis of ALS-FTD. A single amino acid substitution mutation in the mitochondrial protein, coil-coiled-helix-coil-coiled-helix domain containing 10 ($CHCHD10^{S59L}$), leads to familial ALS-FTD. Previously, we demonstrated that the $CHCHD10^{S59L}$ mutation resulted in mitochondrial dysfunction in *Drosophila* and various cell culture models. Axonal mitochondrial transport ensures that mitochondria are transported to high-energy demanding sites, such as synapses, to help aid in synaptic communication. Reduced mitochondrial transport is demonstrated in various neurodegenerative disease models including Alzheimer's disease, Huntington's disease, Parkinson's disease, and other disease mutations of ALS. This suggests that maintaining proper mitochondrial transport is paramount to the health of neurons. Since it is known that the ALS-FTD causing mutation $CHCHD10^{S59L}$ leads to mitochondrial dysfunction, and abnormal mitochondrial transport is present in other neurodegenerative disorders, the goal of this study was to determine if abnormal mitochondrial transport was also present in $CHCHD10^{S59L}$-mediated ALS-FTD. Using a *Drosophila* larval model system and multiple different expression patterns, it was determined that male larvae with 1 copy of the S59L mutation displayed significantly less anterograde mitochondrial movement in the transport parameters flux, distance, and run length. However, there was

no widespread reduction in mitochondrial motility as expected and the majority of the data was inconsistent between the different expression lines. This could suggest that larva have a greater need for mitochondrial motility to support their development, especially the growth of adult specific neurons, and any motility defects that could be present from the S59L mutation, are outweighed by the larva's need for increased mitochondrial motility to support that growth and development. Repeating this project in an adult *Drosophila* system, as well as utilizing an *in vitro* model would help to further elucidate the role, if any, that mitochondrial transport has on the pathogenesis of CHCHD10^{S59L}-mediated ALS-FTD.

Table of Contents

List of Tables

List of Figures

1. Introduction

1.1. Amyotrophic Lateral Sclerosis with Frontotemporal Dementia

Amyotrophic lateral sclerosis (ALS) is a devastating lethal age-progressive motor neuron disease characterized by muscle weakness and loss of function of voluntary muscles. Cognitively, ALS patients remain intact, however, degeneration of both upper and lower motor neurons leads to clinical symptoms such as spasticity, muscle atrophy, impaired walking, and impaired speaking. As the disease progresses, respiratory paralysis also occurs, resulting in death. On average, patients die within two to five years after symptom onset (Boillée et al., 2006). However, there is a wide range of clinical phenotypes, leading others to live ten years or more after diagnosis (Grad et al., 2017), such as the case of Stephen Hawking, who lived for 50 years with ALS. Furthermore, the same gene mutation can result in different clinical manifestations and severity between different people (Al-Chalabi et al., 2014).

The etiology of ALS remains to be elucidated; however, it is likely a complex combination of aging, sex, genetic factors, and environmental factors. For example, military veterans face a higher risk of developing ALS, potentially due to their exposure to toxic metals and chemicals, as well as an increased likelihood of experiencing traumatic brain injuries ("Amyotrophic lateral sclerosis (ALS) - Symptoms and causes," n.d.; Nelson et al., 2018). Additionally, the majority of patients develop ALS between the ages of 45 and 65, and men are more likely to develop the disease than women (Wijesekera and Nigel Leigh, 2009). 90-95% of patients develop ALS without a family history, termed sporadic ALS. Of the 5-10% of patients who develop familial ALS, there

is a high rate of Mendelian inheritance, and most mutations are autosomal dominant, however there is variation in the penetrance of such mutations. Despite the majority of ALS cases occurring sporadically, over 25 causative genes have been identified for familial ALS (Mejzini et al., 2019). Some of the most common mutations occur in genes *SOD1*, *FUS*, and *C9orf72*. There are currently few effective treatments for ALS, and with an aging population, rates of ALS will continue to climb (Akçimen et al., 2023). Therefore, there is a great need to further our understanding of the pathophysiology of this disease to discover new therapies.

Frontotemporal dementia (FTD) is a lethal neurodegenerative disorder characterized by neuronal loss in the frontal and temporal lobe brain regions. FTD is one of the most common form of dementia for people under 65 years of age and is often diagnosed between the ages of 40 and 65 (Galvin et al., 2017). There are several types of FTD, of which, the behavioral variant is the most common (Abramzon et al., 2020; Grad et al., 2017). Symptoms of behavioral FTD include changes in language, behavior, and personality, and the average survival after diagnosis is 3-10 years (Riedl et al., 2014). While the etiology of FTD remains to be completely understood, FTD carries a higher rate of Mendelian inheritance. 25-50% of patients have a family history (Grossman et al., 2023; Rademakers and Hutton, 2007). However, some people with a mutation associated with FTD never develop the disease (incomplete penetrance), once again, highlighting the complex nature of FTD. Similar to ALS, effective therapies for FTD are greatly needed as the disease is estimated to be two times more expensive to the economy than Alzheimer's disease (Galvin et al., 2017).

Interestingly, ALS and FTD are on a continuum and can be diagnosed together because of clinical, genetic, and pathological overlap. Clinically, up to 50% of ALS patients display FTD symptoms, and 15% of ALS patients meet the FTD diagnostic criteria (Nguyen et al., 2018). Similar rates are found in FTD patients displaying motor neuron deficits. Those who meet the diagnostic criteria of both diseases are given the diagnosis of amyotrophic lateral sclerosis with frontotemporal dementia (ALS-FTD). Pathologically, both ALS and FTD are classified as proteinopathy diseases, meaning there is abnormal aggregation of proteins. Namely, ALS and FTD patients have TDP-43 aggregation. Mutations in the ALS-causing gene *TARDBP*, encoding for the protein TDP-43, cause TDP-43 aggregation, however, ALS and FTD patients without this specific gene mutation still display TDP-43 pathology. Up to 97% of ALS patients have TDP-43 aggregation, while up to 50% of FTD patients have the same TDP-43 pathology (Radford et al., 2015). Genetically, there is a wide spectrum of disease mutations associated with ALS, FTD, and ALS-FTD (Figure 1). Some mutations are heavily associated with either ALS or FTD, such as *SOD1* for ALS and *MAPT* for FTD, while others, like *C9orf72* and *CHCHD10*, are associated with ALS-FTD. Mutations in between reflect varying degrees and combinations of ALS and FTD symptoms (Corcia et al., 2017; Ghasemi and Brown, 2018).

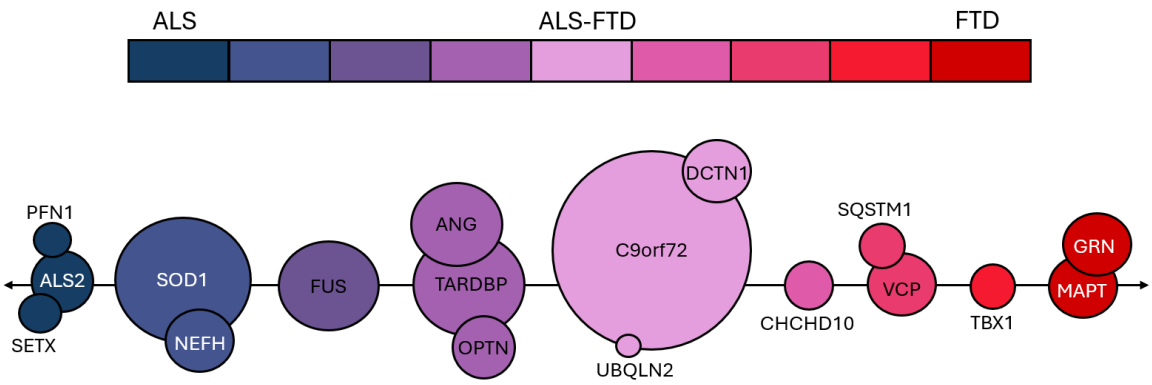

Figure 1: The spectrum of ALS-FTD genetics. Genes very strongly associated with ALS or FTD are furthest to the left or right, respectively. Genes heavily associated with ALS-FTD are depicted in the center. Mutations in between reflect different phenotypic combinations and degrees of ALS and FTD symptoms. Larger circles indicate that gene makes up higher percentages of cases. For example, mutations in C9orf72 account for the majority of familial ALS-FTD cases. Please note that this is not an exhaustive list of genetic mutations.

In 2014, Bannwarth et al. discovered that a single point mutation in the gene *CHCHD10* was a familial cause of ALS-FTD. Coil-coiled-helix-coil-coiled-helix domain containing 10 (CHCHD10) is a protein localized in the inner mitochondrial membrane and plays important roles in maintaining mitochondrial structure (Ajroud-Driss et al., 2015). Bannwarth and colleagues (2014) identified that patients with this single point mutation ($CHCHD10^{S59L}$) had abnormal mitochondrial morphology. In a different study, *Drosophila* and cell culture models with this $CHCHD10^{S59L}$ mutation also exhibited shorter than normal mitochondria, as well as reduced mitochondrial respiration (Baek et al., 2021). Interestingly, other mutations in this same CHCHD10 protein have been identified in a number of other diseases such as Parkinson's disease and Charcot-Marie-Tooth disease (Anderson et al., 2019; Keith et al., 2020), suggesting that defective mitochondria are present in many other diseases.

1.2. Mitochondrial Transport

Mutations in the mitochondrial protein CHCHD10 can lead to a number of diseases. Furthermore, mitochondrial dysfunction is present in many types of neurodegenerative diseases as well as cardiovascular diseases, obesity, cancer, and major depressive disorder (Beal, 2005, 1998; Chistiakov et al., 2018; Ciubuc-Batcu et al., 2024; Nunnari and Suomalainen, 2012), suggesting the importance of maintaining functional mitochondria. Mitochondria are most famously known as the "powerhouse of the cell" because they generate ATP. However, mitochondria also play essential roles in calcium buffering, synaptic communication, metabolism, hormone signaling, and apoptosis (Devine and Kittler, 2018; Jacobs et al., 2020; Kim et al., 2012; Sheng and Cai, 2012).

To ensure mitochondrial function, the mitochondrial quality control (mitoQC) system balances the generation of new mitochondria with the removal of damaged mitochondria. Of particular importance is the degradation of damaged mitochondria. During ATP generation, mitochondria also make reactive oxygen species (ROS) as a by-product. ROS are harmful to mitochondria and can introduce mutations in the mitochondrial genome, creating dysfunctional mitochondria (Fischer et al., 2012). To avoid a buildup of damaged mitochondria, mitochondria get engulfed and recycled, termed mitophagy. The mitoQC system is also important in mitochondrial transport as transport to the correct locations ensures the biogenesis of new mitochondria and the removal of old or damaged mitochondria are balanced (Shanmughapriya et al., 2020). The mitoQC system and mitochondrial transport are also linked, as proteins needed for mitochondrial turnover are also needed for their transport (Dorn, 2021; Misko et al.,

2010). Therefore, a disruption of the mitoQC system has consequences on mitochondrial function and transport.

Mitochondrial transport through a cell ensures that mitochondria are moved to where they are needed, such as high energy-demanding places. Neurons present an additional challenge for mitochondrial transport due to their unique morphology and length. In neurons, mitochondria are transported along microtubules, requiring motor proteins and motor-adaptor complexes (Figure 2). The movement of mitochondria along microtubules is a form of active transport requiring ATP, thus mitochondria provide their own energy for motility. While the majority of mitochondria within a neuron are stationary, motile mitochondria exhibit a dynamic pattern, displaying frequent pauses and oscillations, and extended periods of docking (Lin and Sheng, 2015). Mitochondria also exhibit bi-directional transport or anterograde and retrograde movement. Anterograde transport is the movement of mitochondria towards the axon terminals, or synapses, while retrograde transport is the movement of mitochondria back towards the cell body. Anterograde transport requires the motor protein, kinesin, and additional proteins, such as MIRO and TRAK, to form the motor adaptor complex that provides the connecting bridge between mitochondria and kinesin. Retrograde transport requires the motor protein, dynein, and an additional motor adaptor complex, dynactin (Cai and Sheng, 2009).

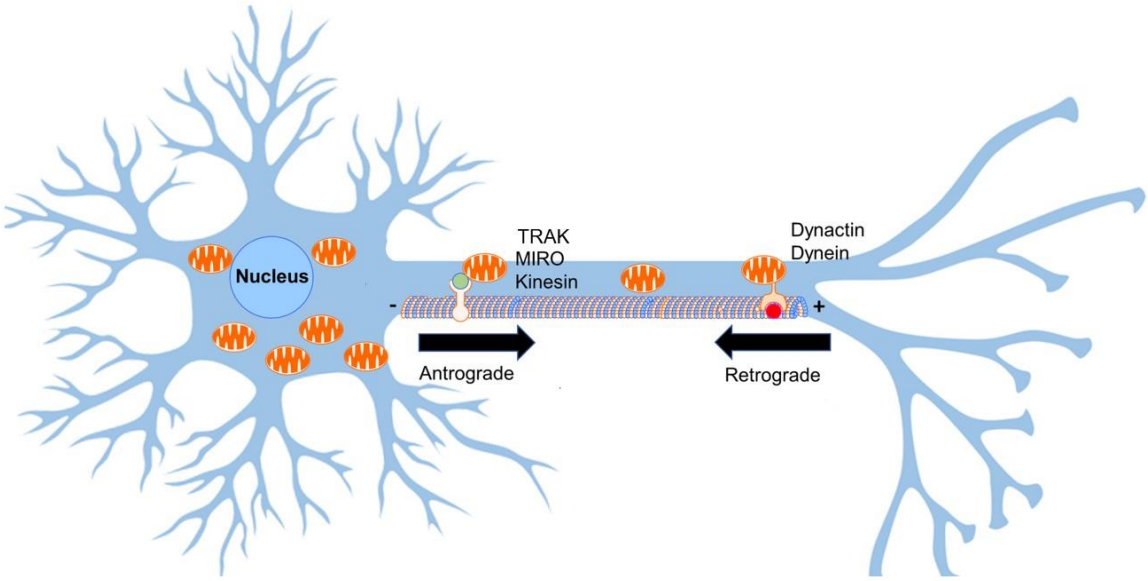

Figure 2: Mitochondrial transport mechanisms through a neuron. Movement towards the axon terminals is anterograde transport, and movement towards the cell body is retrograde transport. Anterograde transport of mitochondria is mediated by the motor protein, kinesin, and motor adaptor complexes, MIRO and TRAK. Retrograde transport of mitochondria is mediated by the motor protein, dynein, and adaptor complex, dynactin. Figure adapted from (Flannery and Trushina, 2019).

Mitochondria are often docked, or anchored, at places that require calcium buffering, or high-energy demanding sites such as Nodes of Ranvier and axon terminals, often to aid in neurotransmission and the growth of new axonal branches (Sheng and Cai, 2012). While it's known that mitochondria dock at places with high levels of intracellular calcium, mediated by MIRO's calcium-sensing motif (Wang and Schwarz, 2009), the mechanism for anchoring mitochondria has been debated. The most likely mechanism is the recruitment of syntaphilin (SNPH) to mitochondria, and its subsequent docking to microtubules, however, the actual physical interactions between SNPH, mitochondria, and the motor proteins remain to be elucidated (Barnhart, 2016; Canty et al., 2023; Chen and Sheng, 2013; Ni et al., 2015). Furthermore, other docking mechanisms, such as

mitochondrial dissociation from microtubules and actin-mediated docking cannot be overlooked (Chang and Reynolds, 2006; Sheng and Cai, 2012).

1.3. Mitochondrial Transport in Health and Disease

Mitochondrial transport is necessary to maintain cellular health by making sure mitochondria are where they are needed when they are needed, and their removal when they are not needed. In the case of neurons, anterograde transport is required to get mitochondria to high energy-demanding places, such as synapses, to help mediate synaptic communication. Synaptic communication, or communication between different neurons, is required for normal brain function. Synaptic communication is mediated by chemical and electrical signals, both of which require ATP. Thus, mitochondria play very large roles in maintaining electrochemical gradients of neurons, as well as mediating synaptic vesicle mobilization, neurotransmitter release, calcium buffering, and vesicle recycling and refilling (Devine and Kittler, 2018). For instance, inhibiting ATP production leads to a decline in neurotransmission (Alnaes and Rahamimoff, 1975). Thus, without synaptic communication, neurons cannot send information to each other, and therefore, cannot mediate things like coordination of movement. On the other hand, retrograde transport is required for removing and degrading damaged mitochondria, as much of the degradation machinery is located near the cell body of a neuron. Thus, if proper transport is not maintained, a neuron's high energy demands won't be met, and damaged mitochondria can accumulate, both of which are toxic to a neuron.

Disruptions in mitochondrial motility are present in a number of diseases and disorders including Alzheimer's disease, Parkinson's disease, Huntington's disease, ALS,

and even schizophrenia and depression (Calkins et al., 2011; Course and Wang, 2016; De Vos et al., 2007; Mattson et al., 2008). In the case of proteinopathy diseases, such as Alzheimer's, Huntington's, and ALS, mutant aggregated proteins often interact with mitochondria, disrupting their transport (Granatiero and Manfredi, 2019; Millecamps and Julien, 2013; Shi et al., 2010; Zheng et al., 2019). Similarly, proteins responsible for mitochondrial transport, such as MIRO, are often targeted by mutant proteins, causing MIRO degradation and reduced mitochondrial motility (Moller et al., 2017).

Reductions of anterograde mitochondrial transport lead to reduced densities of synaptic mitochondria and demonstrated reduced neurotransmission. Interestingly, rescuing mitochondrial transport can ameliorate synapse loss (Calkins et al., 2011; Han et al., 2020; Xie et al., 2015). Therefore, it is plausible to suggest neurons undergo atrophy due to non-homeostatic neurotransmission and contribute to neuronal loss, a hallmark of many neurodegenerative diseases. In fact, neuronal degeneration may even occur before symptom onset in several neurodegenerative disorders (Dadon-Nachum et al., 2011; Devine and Kittler, 2018). Further, a reduction in mitochondrial motility is present before symptom onset in several models of ALS (Magrané et al., 2014; Marinkovic et al., 2012).

Aging is the largest risk factor for developing most age-related neurodegenerative disorders. With an ever-increasing aging population, and few effective treatments, further research is greatly needed. As disruptions in mitochondrial motility are seen across neurodegenerative disorders, therapeutics aimed at restoring mitochondrial transport may prove to be a beneficial target, however, the molecular mechanisms behind disruptions in mitochondrial transport need further elucidation.

1.4. Motivation for Study

Mutations in CHCHD10^{S59L} lead to abnormalities in mitochondrial morphology and function (Baek et al., 2021; Bannwarth et al., 2014), and dysfunctional mitochondria are seen in many neurodegenerative diseases. Furthermore, abnormal mitochondrial transport is also present in neurodegenerative disease models, including disease mutations in ALS. Since it is known that mitochondrial dysfunction is present in CHCHD10^{S59L}, the goal of this study was to determine if abnormal mitochondrial transport was also present in CHCHD10^{S59L}-mediated ALS-FTD. The hypothesis was neurons displaying the CHCHD10^{S59L} mutation would exhibit abnormal mitochondrial transport, leading to toxicity in these motor neurons. Based on previous literature, we expected to see a decrease in mitochondrial trafficking, however, mitochondrial transport has not been studied in this specific mutation. Therefore, the present study may help elucidate the role of mitochondrial transport in the pathogenesis of CHCHD10^{S59L}-mediated ALS-FTD. To achieve this goal, several model systems were tested, and the *Drosophila* larval system was established to investigate the effect of CHCHD10^{S59L} on axonal mitochondrial transport.

2. Methods

2.1. Cell Differentiation and Transient Transfection

SH-SY5Y cells were plated at $3.0x10^5$ cells in a 35 mm dish in DMEM/F12 containing FBS (10%v/v). Plates were incubated overnight at 37℃ with 5% CO_2 to allow for cell adhesion. Standard media was removed and replaced with differentiation media: DMEM/F12 containing FBS (1%v/v) and 10 µM of retinoic acid (RA). This was considered Day 1. On Day 4 the differentiation media was refreshed. On Day 7, after confirmation of successful differentiation, transient transfection was performed using NeuroMag (OZ Biosciences). 4 µg of plasmid DNA (4 µg EV; 2 µg $CHCHD10^{WT}$-GFP11 + 2 µg MTS-GFP 1-10; 2 µg $CHCHD10^{S59L}$-GFP11 + 2 µg MTS-GFP 1-10) was diluted in 12 µl of NeuroMag Reagent and 184 µl of medium without serum. The DNA/NeuroMag complex was incubated for 15 minutes at room temperature. After incubation, the complex was added directly to the differentiated plate. The differentiated plate was placed on a magnetic plate and incubated for 15 minutes. The plate was removed from the magnet and placed in the CO_2 incubator for 24 hours prior to imaging.

2.2. **Drosophila** *Genetics and Generation of Lines*

The motoneuron driver OK371, and the mitochondrial marker, UAS>mito-GFP were used to fluorescently visualize mitochondria in larval motor neurons. Flies carrying OK371, UAS>mito-GFP were crossed with flies either expressing the control protein, CG5010 WT, or CG5010 S81L. CG5010 is the fly ortholog to human CHCHD10, therefore CG5010 WT is WT CHCHD10 and CG5010 S81L is CHCHD10 S59L.

Fly cultures and crosses were performed on Bloomington Stock Center standard cornmeal food at 25℃. Initial genotypes used for genetic crosses are shown in Table 1. CG5010 (C2C10H herein after) transgene generation was previously described in Baek et al. 2021. Final genotypes used for dissections are shown in Table 2.

To generate the heterozygous control line, virgin females carrying OK371, UAS>mito-GFP/CyO-YFP; UAS>CD8-RFP/CD8-RFP (genotype 1 in Table 1) were crossed with males carrying w^{1118} (wild-type, genotype 2 in Table 1) (Figure 3 A). Progeny without YFP were collected for dissections (Table 2). To generate the homozygous control line, virgin females carrying the genotype 1 construct were crossed with males also carrying the genotype 1 construct (Figure 3 B). To ensure only 1 copy of the driver OK371 was present, progeny with GFP and YFP were collected for dissections (Table 2). To generate the double homozygous control line, virgin females carrying OK371/OK371; +/+ (genotype 5 in Table 1) were crossed with males carrying the genotype 1 construct (Figure 3 C). To ensure 2 copies of the driver OK371 were present, progeny without YFP were collected for dissection (Table 2).

To generate the heterozygous C2C10H WT line, laboratory fly stocks were used to create 2 separate lines, Bl/CyO-YFP; TM2/TM6 and OK371, UAS>mito-GFP/CyO-YFP; CD8-RFP/TM6, both of which were needed for downstream mating. Virgin females carrying pUAST-C2C10H_FLAG #1-3 (attp2)/TM3 (genotype 3 in Table 1) were crossed with males carrying the Bl/CyO-YFP; TM2/TM6 construct. Progeny with the genotypes Bl/+; WT/TM2 and CyO-YFP/+; WT/TM6 were crossed together to obtain Bl/CyO-YFP; WT/TM6 (F2 progeny). Virgin females carrying the OK371, UAS>mito-

GFP/CyO-YFP; CD8-RFP/TM6 construct were then crossed with male F2 progeny. Progeny with the genotype OK371, UAS>mito-GFP/CyO-YFP; WT/TM6 were collected (F3 progeny). F3 progenies were crossed together to make a stable line for further mating. Finally, virgin female F3 progeny were crossed with males carrying the genotype 2 construct (Figure 3 D). Progeny without YFP and TM6 were collected for dissections (Table 2). To generate the homozygous C2C10H WT line, virgin female and male stable line F3 progeny were mated (Figure 3 E). Once again, to ensure only 1 copy of OK371 was present, progeny expressing GFP and YFP were collected for dissections (Table 2). To generate the double homozygous C2C10H WT line, virgin females carrying OK371/CyO; pUAST-C2C10H_FLAG #1-3/TM2 (genotype 6 in Table 1) were crossed with males expressing OK371, UAS>mito-GFP/CyO-YFP; WT/TM6 (stable line F3 progeny) (Figure 3 F). Progeny without YFP were collected for dissections (Table 2).

Finally, to generate the heterozygous C2C10H S81L line, virgin females carrying pUAST-C2C10H S81L_FLAG #2-3 (attp2)/TM3 (genotype 4 in Table 1) were crossed with males carrying the Bl/CyO-YFP; TM2/TM6 construct. Progeny with the genotypes Bl/+; S81L/TM2 and CyO-YFP/+; S81L/TM6 were crossed together to obtain Bl/CyO-YFP; S81L/TM6 (F2 progeny). Virgin females carrying the OK371, UAS>mito-GFP/CyO-YFP; CD8-RFP/TM6 construct where crossed with male F2 progeny. Progeny with the genotype OK371, UAS>mito-GFP/CyO-YFP; S81L/TM6 were collected (F3 progeny). Again, F3 progenies were crossed together to make a stable line for further mating. Finally, virgin female F3 progeny were crossed with males carrying the genotype 2 construct (Figure 3 G). Progeny without YFP and TM6 were collected for dissections

(Table 2). To generate the homozygous C2C10H S81L line, virgin female and male stable line F3 progeny were mated (Figure 3 H). Once again, to ensure only 1 copy of OK371 was present, progeny expressing GFP and YFP were collected for dissections (Table 2). To generate the double homozygous C2C10H S81L line, virgin females carrying OK371/CyO; pUAST-C2C10H S81L_FLAG #2-3/TM6 (genotype 7 in Table 1) were crossed with males carrying OK371, UAS>mito-GFP/CyO-YFP; S81L/TM6 (stable line F3 progeny) (Figure 3 I). Progeny without YFP were collected for dissections (Table 2).

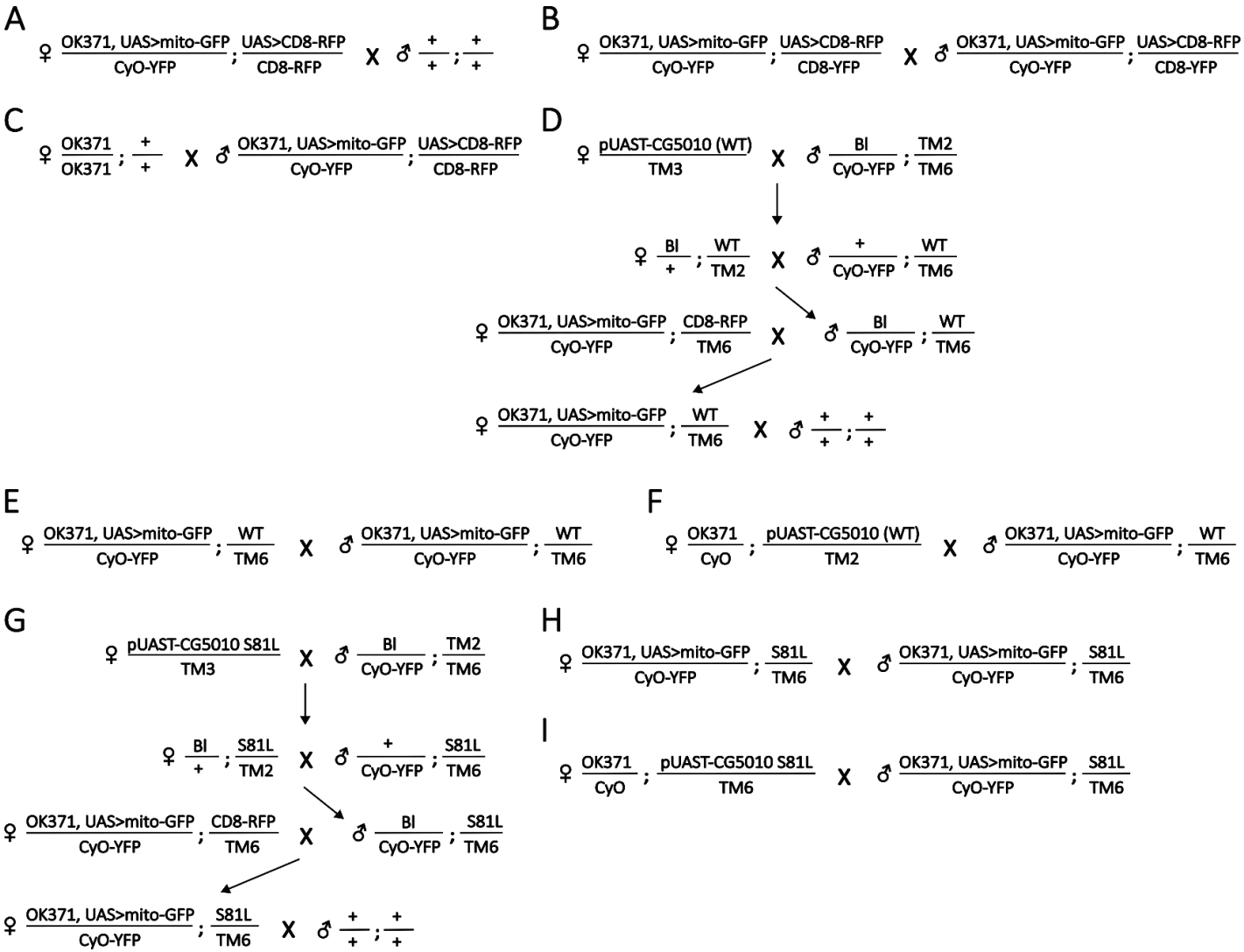

Figure 3: Mating schemes for the generation of heterozygous, homozygous, and double homozygous models. (A) Heterozygous control. **(B)** Homozygous control. **(C)** Double homozygous control. **(D)** Heterozygous WT. **(E)** Homozygous WT. **(F)** Double homozygous WT. **(G)** Heterozygous S81L. **(H)** Homozygous S81L. **(I)** Double homozygous S81L.

Table 1: Initial genotypes used for mating schemes. Genotypes 2 and 5 are from Bloomington Stock Center (#5905, #26160, respectively). All other genotypes were made in house. Mito-GFP (#8442), CD8-RFP (#32218), and CyO-YFP (#8578) constructs were initially obtained from Bloomington Stock Center.

Genotype
1. OK371, UAS>mito-GFP/CyO-YFP; UAS>CD8-RFP/CD8-RFP
2. w^{1118} (+/+; +/+)
3. pUAST-C2C10H_FLAG #1-3 (attp2)/TM3
4. pUAST-C2C10H S81L_FLAG #2-3 (attp2)/TM3
5. OK371/OK371; +/+
6. OK371/CyO; pUAST-C2C10H_FLAG #1-3/TM2
7. OK371/CyO; pUAST-C2C10H S81L_FLAG #2-3/TM6

Table 2: Final genotypes used for dissections. Heterozygous animals have 1 copy of OK371 and 1 copy of the transgene (control, WT, or S81L). Homozygous animals have 1 copy of OK371 but have 2 copies of the transgene. Double homozygous animals have 2 copies of OK371 and 2 copies of the transgene.

Heterozygous	Homozygous	Double Homozygous	Explanation
OK371, UAS>mito-GFP/+; UAS-CD8-RFP/+	OK371, UAS>mito-GFP/CyO-YFP; UAS-CD8-RFP/UAS-CD8-RFP	OK371, UAS>mito-GFP/OK371; UAS-CD8-RFP/+	Used as a control for CHCHD10 WT and S81L overexpression
OK371, UAS>mito-GFP/+; pUAST-C2C10H/+	OK371, UAS>mito-GFP/CyO-YFP; pUAST-C2C10H/pUAST-C2C10H	OK371, UAS>mito-GFP/OK371; pUAST-C2C10H/pUAST-C2C10H	Used to evaluate CHCHD10 overexpression function on mitochondrial transport
OK371, UAS>mito-GFP/+; pUAST-C2C10H S81L/+	OK371, UAS>mito-GFP/CyO-YFP; pUAST-C2C10H S81L/pUAST-C2C10H S81L	OK371, UAS>mito-GFP/OK371; pUAST-C2C10H S81L/pUAST-C2C10H S81L	Used to evaluate mutant CHCHD10 function on mitochondrial transport

2.3. Larval Dissections

Larval dissections were performed according to (Neisch et al., 2016). To quantify mitochondrial transport along motor neurons, ten (five male and five female) wandering third-instar larvae for each genotype were collected, washed in water, and pinned on a Sylgard dish at the anterior and posterior ends, dorsal side up. The sample was

submerged in modified HL3.1 media (70 mM NaCl, 5 mM KCl, 1.5 mM $CaCl_2$, 4 mM $MgCl_2$, 10 mM $NaHCO_3$, 5 mM Trehalose, 115 mM Sucrose, 5 mM HEPES, pH adjusted to 7.4). A single cut through the dorsal top layer was made perpendicular to the posterior end. Scissors were inserted into the incision and used to cut through the dorsal wall along the body towards the anterior end. Two pins were used to anchor the anterior edges of the body wall, and an additional two pins were used to anchor the posterior edges of the body to splay open the larva. Forceps were used to detach the hindgut, proventriculus, and tracheal dorsal trunk tubes from the larva. All tissue was removed except for the brain, axons, and anterior body wall muscles. The modified HL3.1 media was replaced with fresh media to cover the larva in a thin layer. A No. 1.5 coverslip was placed across the sample and gently pressed down to be even with the top of the Sylgard slide.

2.4. Mitochondrial Imaging

The use of the driver OK371, UAS>mito-GFP allows for fluorescent visualization of mitochondria. Larva were live imaged using the Nikon Crest X-light 2 Spinning Disc confocal microscope on the SIL100x objective (1.35 NA). The ventral ganglion was visualized first to set orientation so that mitochondria moving in the anterograde direction were traveling left to right. Time lapses were set for three minutes, with an image capture every one second. The laser power was set to 10% power and FITC exposure (498 nm excitation, 517 nm emission) set to 200 ms to avoid photobleaching of the samples.

2.5. Immunoblotting

Samples were collected and lysed in RIPA buffer (Cell Signaling Technology) containing a protease inhibitor cocktail (Sigma). Proteins were separated by either SurePAGE, Bis-Tris, 4-12% or ExpressPlus PAGE, 4-12% gels (GenScript) and then transferred to a nitrocellulose membrane using the iBlot 2 Mini system (ThermoFisher). Membranes were blocked using LI-COR blocking buffer for one hour. Primary antibodies were diluted in 0.2% Tween 20 in LI-COR blocking buffer and incubated overnight. Membranes were washed three times for 10 minutes using 1x TBST (0.1% Tween 20 detergent in tris-buffered saline) and then secondary antibodies were diluted in 0.2% Tween 20 in LI-COR blocking buffer and incubated for one hour. Membranes were washed with 1x TBST three times for ten minutes. Immunoblots were visualized with the Odyssey FC System (LI-COR). The following primary antibodies were used: FLAG (Proteintech, 1:20,000), Actin (Santa Cruz Biotechnology, 1:1,000). Secondary antibodies were fluorophore-conjugated species-specific (LI-COR, 1:10,000).

2.6. Image Analysis and Statistical Analysis

To understand the transport behavior of mitochondria, the following transport parameters were analyzed: flux, percentage of total mitochondrial movement, velocity, distance, run length, and duty cycle. The software Fiji was used with or without the MTrackJ plugin. MTrackJ was chosen over some of the other manual software (e.g., TrackMate) for its ease of use and for its more detailed numerical outputs. MTrackJ was used to measure velocity, distance, run length, and duty cycle. Only mitochondria that

were present for at least 60 frames were chosen, and a minimum of 10 mitochondria were tracked per sample. The anterior end of a mitochondrion was tracked as it is more reliable than tracking the center of a mitochondrion (Louie et al., 2008). After measuring, MTrackJ outputs two Excel files, a Tracks file and a Points file. The Tracks file gives broader assessments of movement such as average distance and average velocity. The Points file breaks down each track into each point and allows for more detailed assessment of movements such as run length and duty cycle.

Flux

Flux gives the best indication of overall movement of mitochondria within an axon as it determines how many mitochondria arrive at a particular point, regardless of how they behaved to get to that point. To measure flux, a single line was drawn in the center of the axon and the number of mitochondria that crossed that line were counted for the entire movie. Anterograde moving mitochondria and retrograde moving mitochondria were counted separately. The final numbers were divided by 3 so that units of flux were mitochondrial flux/min.

Percentage of Total Mitochondrial Movement

Percentage of total mitochondrial movement describes the percentage of all mitochondria that are stationary, the percentage that move in the anterograde direction, and the percentage that move in the retrograde direction. The Cell Counter plugin in Fiji was used to mark stationary mitochondria in Category 1, anterograde mitochondria in Category 2, and retrograde mitochondria in Category 3. Categories 1, 2, and 3 were totaled to get the total amount of mitochondria in an axon and then each category was

divided by the total number of mitochondria to obtain the percentage of total mitochondrial movement.

Velocity and Distance

Velocity measures how fast a mitochondrion travels. MTrackJ measures velocity during each point and gives an average in the Tracks file. Distance measures how far a mitochondrion travels. MTrackJ measures the displacement between each point and adds them up to give a total distance traveled in the Tracks file.

Run Length

Run length describes the persistence of transport. A run is defined by periods of movement bounded by pauses. To measure the number of runs, a run was specifically defined as periods of movement greater than + 0.1 μm or less than - 0.1 μm for a minimum of 3 consecutive frames. To calculate the number of runs, the difference in distance between displacement points was used from the Points file. For example, point 1 was subtracted from point 0, and point 2 was subtracted from point 1, and so on. To determine the average run length for a mitochondrion, the total distance traveled was divided by the number of runs.

Duty Cycle

Duty cycle describes the percentage of time a single mitochondrion spends either stationary, moving in the anterograde direction, or moving in the retrograde direction. To calculate the duty cycle, the difference in distance between points was used, exactly like run lengths. A change of 0 was classified as stationary, anything above 0 was considered anterograde, and anything below 0 was considered retrograde. For each mitochondrion,

the number of 0s was tallied. Anything above 0 and anything below 0 were tallied independently. To determine the percentage of time a mitochondrion spent stationary, the total number of 0s was divided by the total tallies of stationary, anterograde, and retrograde motion added together. This step was repeated to determine the percentage of time the mitochondrion spent moving anterogradely and retrogradely.

Statistical Analysis

Analysis of variance (ANOVA) with Dunnett's post hoc was used to test statistical significance. Males and females were analyzed separately. Further, due to the separate functions of anterograde movement and retrograde movement, net anterograde mitochondria were analyzed separately from net retrograde mitochondria. All p values $\leq$ 0.05 were considered statistically significant.

3. Results

3.1. Experimental System Setup

To investigate mitochondrial transport in CHCHD10^{S59L}-mediated ALS-FTD, several different model systems were evaluated. One of them was an *in vitro* SH-SY5Y model. SH-SY5Y cells are derived from human neuroblastoma and can be differentiated into cells displaying mature neuron-like features such as reduced proliferation, expression of neuronal markers, and of particular importance, the formation and extension of neurites (de Medeiros et al., 2019; Shipley et al., 2016). The formation and extension of neurites allow us to study mitochondrial motility along the length of an axon, thus this cell line was most appropriate for the present study. There are several different methods for differentiation required to turn immature SH-SY5Y cells into a mature neuron-like cell. In this study, a simple and widely used differentiation method was utilized (1% FBS, 10 µM RA in DMEM/F12). Unfortunately, consistent differentiation of SH-SY5Y cells was unsuccessful. Successful differentiation is distinguished by numerous neurite extensions; conversely, on day 7, unsuccessful differentiation is characterized by minimal neuronal processes and a predominance of flat cell morphology (Figure 4). If cells are differentiating as they should be, neurites can even be seen by day 3 (Figure 4).

During the first period of overall successful differentiation, mitochondrial movement was observed in differentiated SH-SY5Y cells, however there was inconsistency during this period in differentiation efficacy. After several successful and unsuccessful attempts using 10 µM RA in 1% FBS DMEM/F12, the differentiation media was adjusted to include brain-derived neurotrophic factor (BDNF), as this can aid in

differentiation (Encinas et al., 2000). Several other adjustments were made, including changing the media recipe for the normal culture of SH-SY5Y cells (undifferentiated media), and even obtaining a different stock of SH-SY5Y cells from another lab as the morphology and proliferation rate of the original SH-SY5Y cells used changed drastically. A potential reason for the difference between lab stocks is the media the cells are cultured in. The undifferentiated media was adjusted from 20% FBS in DMEM to 10% FBS in DMEM/F12 due to the change in SH-SY5Y morphology and proliferation rate. DMEM/F12 is the typical media used for SH-SY5Y culture, but DMEM can also be used, and may even be better for proliferation than DMEM/F12 (Sakagami et al., 2017). Because of this, and because DMEM was what the Kim lab had more readily available, DMEM was chosen as the undifferentiated media at the beginning of the present study. However, the other lab that provided the stock of SH-SY5Y cells used DMEM/F12 undifferentiated media. After several bouts of inconsistent differentiation efficiency, SH-SY5Y cells were cultured side by side in the two different medias. Cells grown in 20% FBS in DMEM had slower proliferation rates compared to cells grown in 10% FBS in DMEM/F12 (data not shown). To confirm this, the stock from the other lab was also grown side by side in the two different medias. Over several weeks, the SH-SY5Y cells grown in 20% FBS in DMEM transformed into having larger cell morphology, slower proliferation, and had minimal differentiation compared to the SH-SY5Y cells grown in 10% FBS in DMEM/F12 (data now shown). Thus, it appeared the differentiation issues were in part caused by the media. However, after several months of successful differentiation, the acquired SH-SY5Y cells grown in 10% FBS in DMEM/F12 also

started to not differentiate consistently, thus the undifferentiated media was not the only reason. Due to time constraints and inconsistent differentiation, further optimization was not pursued, and thus, SH-SY5Y cells ultimately were not utilized in this study.

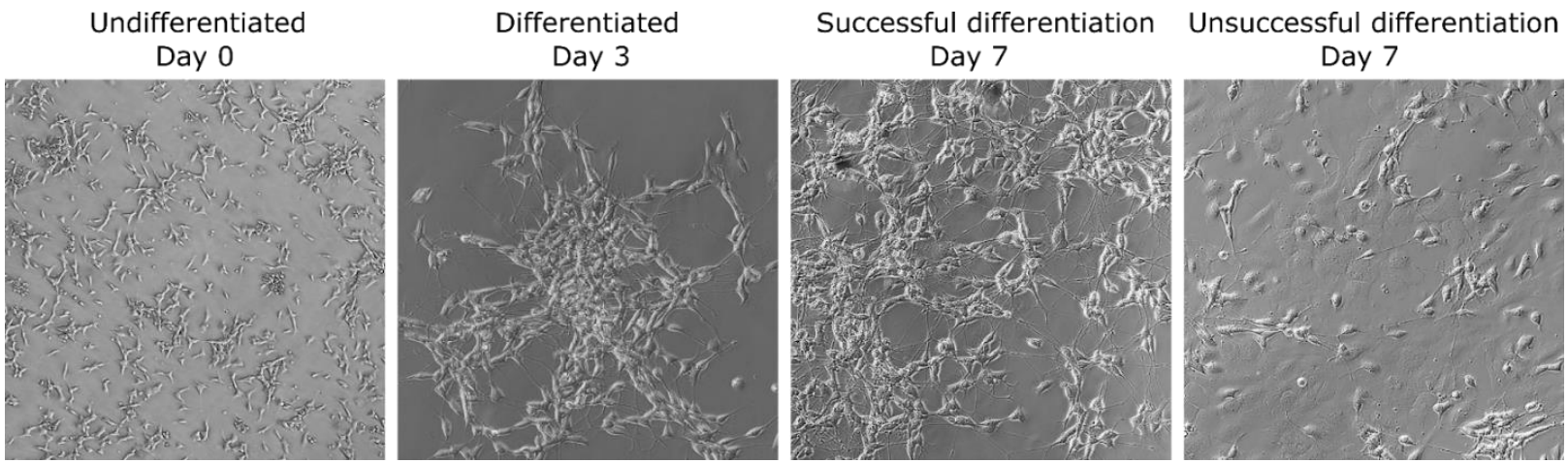

Figure 4: Differentiation of SH-SY5Y cells to induce a neuron-like phenotype. Undifferentiated SH-SY5Y cells are plated on Day 0 (farthest left panel). Differentiation is induced on Day 1 by reducing the FBS concentration to 1% and adding 10 µM of RA. Differentiation can be seen by Day 3 (second panel from the left). The differentiation media is replaced on Day 3. By Day 7, differentiation is distinguished by numerous neurite extensions (third panel from the left). Unsuccessful differentiation of SH-SY5Y cells on Day 7 is marked by a lack of neurite processes and flat cell morphology (furthest right panel).

A second model evaluated was the adult *Drosophila* wing model. This is an age-related model, and therefore, is more representative of the human ALS-FTD population, thus we thought this would be the most appropriate model to use for the present study. Briefly, this model involved anesthetizing a fruit fly before using glycerol and double-sided tape to adhere the fly to a coverslip. A second coverslip was put over the top to enclose the sample. One difficulty of this model was due to the curvature of the wing to the body. Mitochondria can be visualized best in the L1, costal, or L3 regions of an adult fruit fly wing (Figure 5 A). However, due to the wing curvature to the body, clear live images with the entire segment in view proved difficult (Figure 5 B). Furthermore, to prevent the fly from moving around during imaging, the coverslips had to be close together, however, if they were too close together, the fly was crushed. This resulted more often than not, in no mitochondrial movement. Therefore, due to this cruder methodology and less established protocol, the adult fly model was not utilized in the present study.

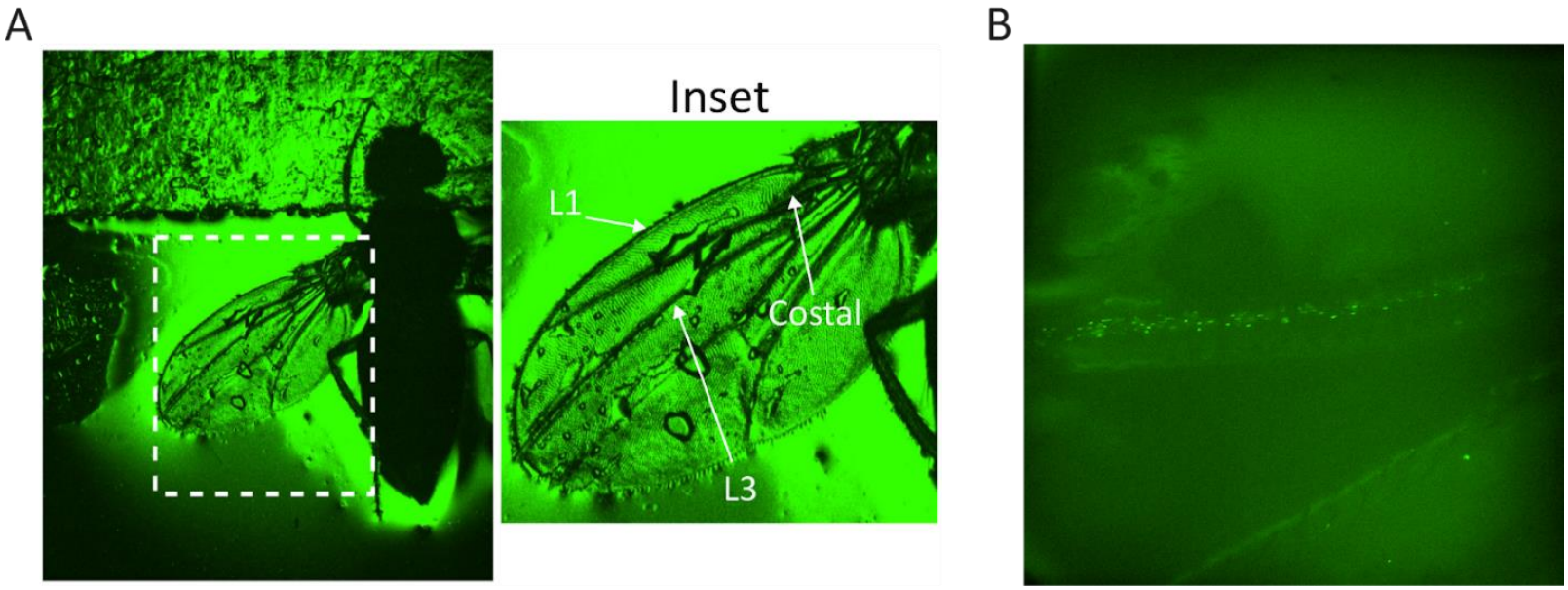

Figure 5: Adult *Drosophila* wing model setup. (A) A 4x microscope image of the adult wing setup. The adult fly head is placed on a layer of double-sided tape. To adhere the wing to the coverslip, glycerol was brushed over the wing. An inset image shows a zoomed-in view of the same wing labeling L1, costal, and L3 wing regions where mitochondria can be visualized for imaging. **(B)** A 100x microscope image of the costal vein. Due to the curvature of the wing, the entire costal vein is not in view, making mitochondrial tracking inaccurate.

The third, and final system, was the *Drosophila* larva model. This model is considerably more established than the adult wing model and is well established across the fly community (Devireddy et al., 2014). This model is also less time consuming, as this model does not require the aging of flies like the adult model does. Therefore, based on consistency, skill, protocol establishment, and timing, the larva model was chosen for the present study.

3.2. Mitochondrial Transport in Drosophila *Larva*

To evaluate mitochondrial transport in the pathogenesis of CHCHD10^{S59L}-mediated ALS-FTD, the *Drosophila* GAL4/UAS system was utilized. GAL4 is under the control of a tissue-specific enhancer, therefore GAL4 determines where the transgene will be expressed in the body. The transgene is under the control of UAS, therefore UAS determines what transgene is expressed. In the present study, the motoneuron driver OK371, and the mitochondrial marker, UAS>mito-GFP were used to fluorescently visualize mitochondria in larval motor neurons. Flies carrying OK371, UAS>mito-GFP were crossed with flies either expressing the control protein, C2C10H WT, or C2C10H S81L. The control protein for the present study was CD8-RFP which labels membranous structures with red fluorescence protein. Paired with OK371, CD8-RFP therefore, labels motor neurons with RFP. C2C10H is the fly ortholog to human CHCHD10, therefore C2C10H WT is WT CHCHD10 and C2C10H S81L is CHCHD10 S59L. From now on C2C10H WT and C2C10H S81L will be shortened to WT and S81L, respectively.

Three different genotype models were used in the present study: a heterozygous model, a homozygous model, and a double homozygous model. The heterozygous model

carries 1 copy of OK371 and 1 copy of the transgene (i.e., control, WT, or S81L). The homozygous model carries 1 copy of OK371 and 2 copies of the transgene. The double homozygous model carries 2 copies of OK371 and 2 copies of either WT or S81L. The double homozygous control line has 2 copies of OK371, but only 1 copy of the control protein. Only 1 copy of the control protein was used due to technical limitations. To avoid confusion, heterozygous lines may be referred to as 1(x) copy and homozygous lines may be referred to as 2(x) copies.

Protein expression of S81L and WT were confirmed in the larval fly system using a Western blot (Figure 6). S81L and WT constructs are FLAG tagged, thus an anti-FLAG antibody was used to confirm the presence of S81L and WT in their respective lines. As expected, the homozygous expression of S81L and WT led to a higher band intensity compared to the heterozygous expression of S81L and WT.

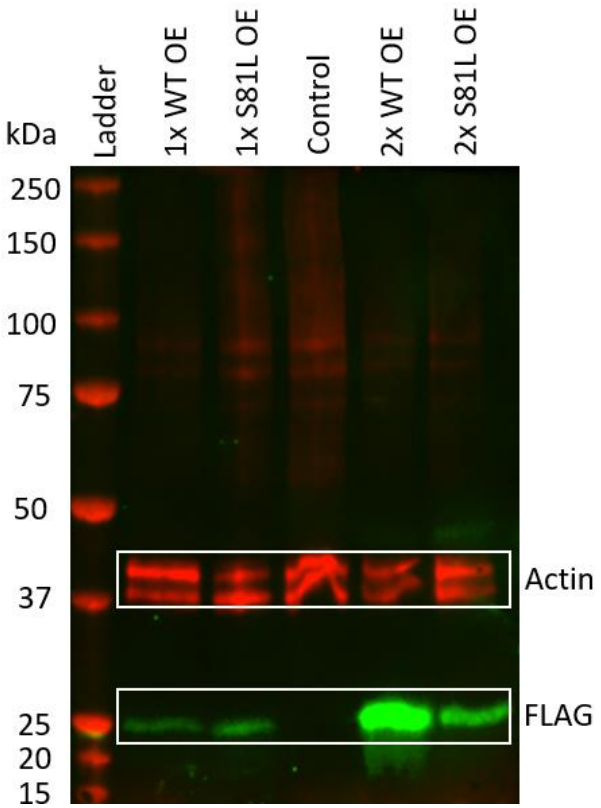

Figure 6: Western blot confirmation of protein expression. 1x is heterozygous and 2x is homozygous.

3.2.1. Flux

Male Flux

In motor neurons expressing the S81L mutation, we expected to see a decrease in mitochondrial transport. Based on Baek's study, we also expected to see an increase in mitochondrial transport in WT expressing motor neurons due to its protective effects. Parameters with statistically significant data will have averages displayed in the text. All other parameters are not statistically significant. Trends of statistically nonsignificant data with small p-values will be included with their p-values and absolute effect size (AES) stated in parentheses (Visentin et al., 2020), but their averages will not be included in the text. All averages, standard deviations, and p-values for flux are provided in Table

3. The average anterograde flux for 1 copy of S81L in males was 2.53 mitochondria/min, while the average anterograde flux for the control group was 4.27 mitochondria/minute, thus 1 copy of S81L resulted in significantly reduced movement in the anterograde direction (Figure 7 A, D; Table 3).

Contrary to our expectations, mitochondria with 1 copy of WT trended towards decreased flux in the anterograde compared to the control, but it was not statistically significant ($p = 0.0791$, AES: 1.40) (Figure 7 A, D; Table 3). Double homozygous WT male mitochondria trended towards increased anterograde flux compared to the control, but it was also not statistically significant ($p = 0.239$, AES: 1.60) (Figure 7 C, F; Table 3). 1 copy of S81L or WT expression did not result in a statistically significant difference in retrograde flux (Figure 7 A, G; Table 3). Similarly, homozygous S81L and WT mitochondria did not display significant differences in anterograde flux or retrograde flux compared to the control (Figure 7 B, E, H; Table 3). Double homozygous S81L expression did not lead to significant differences in anterograde or retrograde flux compared to the control (Figure 7 C, F, I; Table 3). Double homozygous WT expression also did not lead to a significant difference in retrograde flux compared to the control (Figure 7 C, I; Table 3).

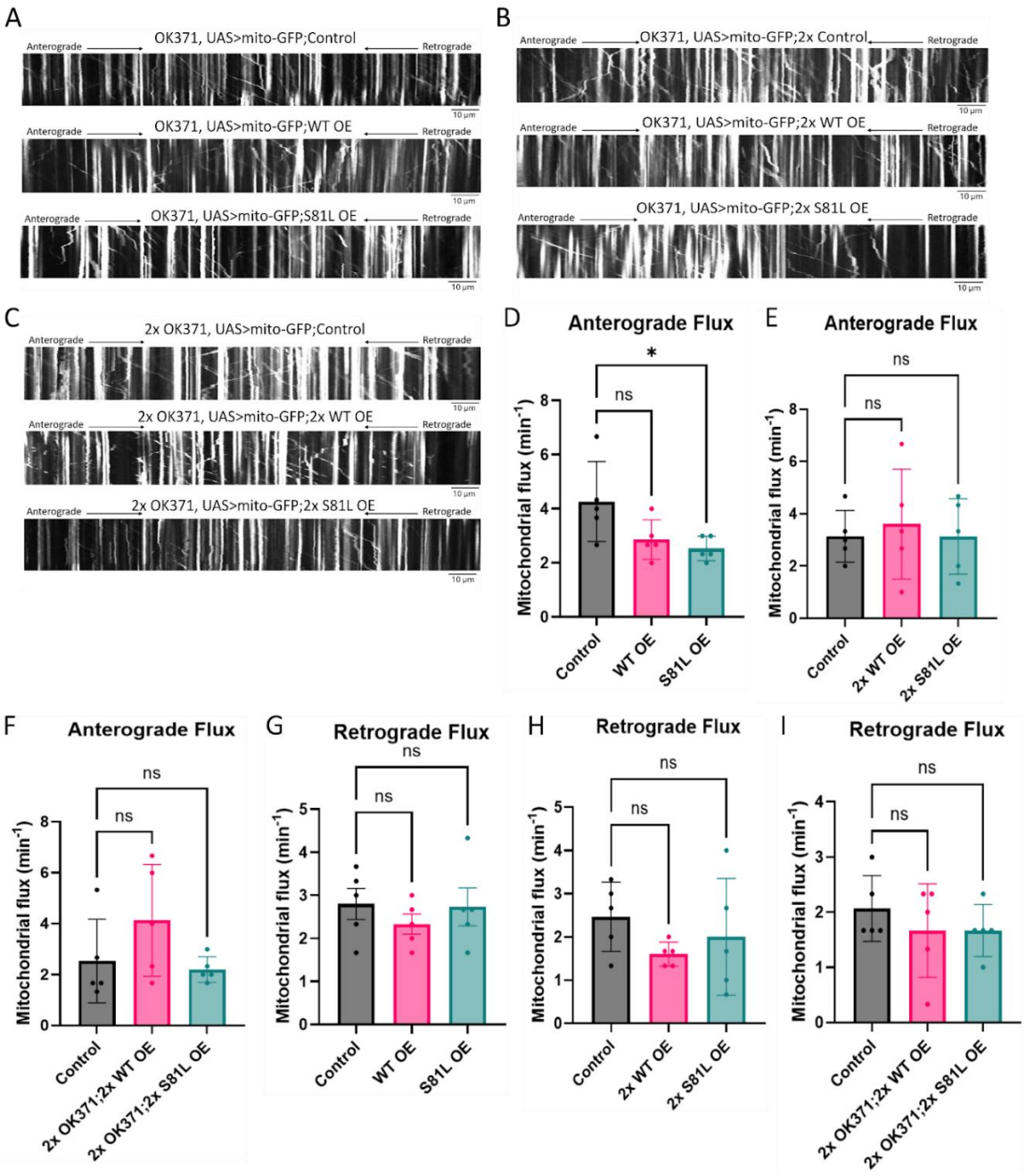

Figure 7: Mitochondrial flux in male larvae. (A) Kymographs of heterozygous males. Top kymograph is the control, middle kymograph is WT, and the bottom kymograph is S81L. **(B)** Kymographs of homozygous males. Top kymograph is the control, middle kymograph is WT, and the bottom kymograph is S81L. **(C)** Kymographs of double homozygous males. Top kymograph is the control, middle kymograph is WT, and the bottom kymograph is S81L. **(D)** Quantification of anterograde flux for heterozygous males. **(E)** Quantification of anterograde flux for homozygous males. **(F)** Quantification of anterograde flux for double homozygous males. **(G)** Quantification of retrograde flux for heterozygous males. **(H)** Quantification of retrograde flux for homozygous males. **(I)** Quantification of retrograde flux for double homozygous males. Data are shown as mean ± SD. NS: not significant. * $p < 0.05$.

Table 3: Male flux averages ± standard deviation (p-value).

Parameter	Experimental Group	Heterozygous	Homozygous	Double Homozygous
Anterograde Flux				
	Control	4.27 ± 1.48	3.13 ± 0.989	2.53 ± 1.64
	WT OE	2.87 ± 0.730 (0.079)	3.60 ± 2.10 (0.856)	4.13 ± 2.19 (0.239)
	S81L OE	2.53 ± 0.447 (0.031)	3.13 ± 1.45 (1.00)	2.20 ± 0.506 (0.925)
Retrograde Flux				
	Control	2.80 ± 0.803	2.47 ± 0.803	2.07 ± 0.596
	WT OE	2.33 ± 0.527 (0.565)	1.60 ± 0.279 (0.272)	1.67 ± 0.850 (0.545)
	S81L OE	2.73 ± 0.983 (0.987)	2.00 ± 1.35 (0.649)	1.67 ± 0.471 (0.545)

Female Flux

All flux averages, standard deviations, and p-values are provided in Table 4. Overall, there were no statistically significant differences in flux in either anterograde or retrograde directions between the groups and across expression lines in females, however, 1x S81L mitochondria trended towards increased movement in the anterograde direction compared to the control ($p = 0.1504$, AES: 1.54) (Figure 8 A, D; Table 4). Similarly, double homozygous S81L anterograde mitochondria also trended towards increased movement compared to the control ($p = 0.2646$, AES: 1.60) (Figure 8 C, F; Table 4). For anterograde flux, there were no significant differences between homozygous S81L, heterozygous WT, homozygous WT, and double homozygous WT and the control (Figure 8 A, B, C, D, E, F; Table 4). For retrograde flux, there were no significant differences between heterozygous S81L and WT, homozygous S81L and WT, and double homozygous S81L and WT and the control (Figure 8 A, B, C, G, H, I; Table 3).

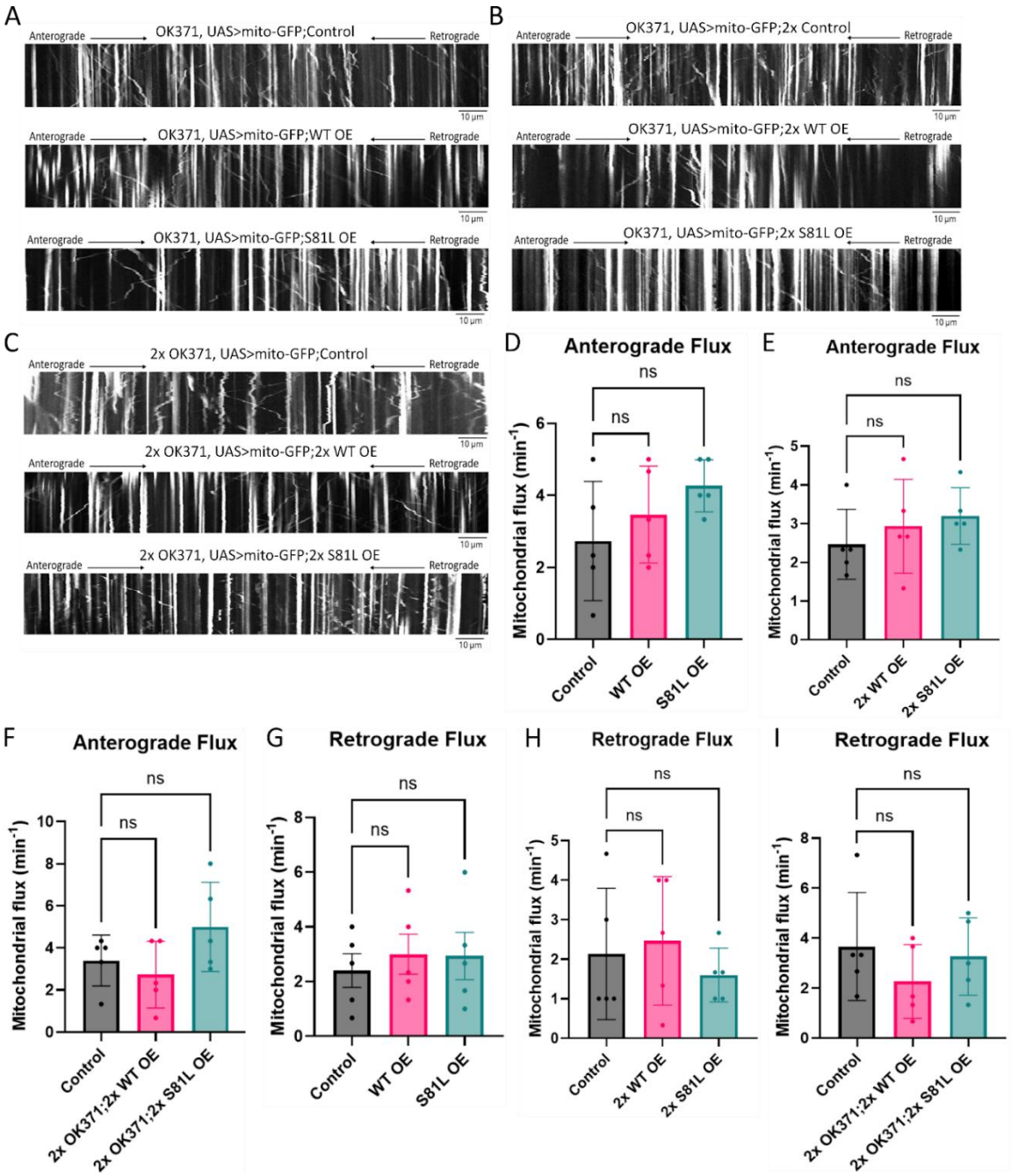

Figure 8: Mitochondrial flux in female larvae. (A) Kymographs of heterozygous females. Top kymograph is the control, middle kymograph is WT, and the bottom kymograph is S81L. **(B)** Kymographs of homozygous females. Top kymograph is the control, middle kymograph is WT, and the bottom kymograph is S81L. **(C)** Kymographs of double homozygous females. Top kymograph is the control, middle kymograph is WT, and the bottom kymograph is S81L. **(D)** Quantification of anterograde flux for heterozygous females. **(E)** Quantification of anterograde flux for homozygous females. **(F)** Quantification of anterograde flux for double homozygous females. **(G)** Quantification of retrograde flux for heterozygous females. **(H)** Quantification of retrograde flux for homozygous females. **(I)** Quantification of retrograde flux for double homozygous females. Data are shown as mean ± SD. NS: not significant.

Table 4: Female flux averages ± standard deviation (p-value).

Parameter	Experimental Group	Heterozygous	Homozygous	Double Homozygous
Anterograde Flux				
	Control	2.73 ± 1.66	2.47 ± 0.901	3.40 ± 1.21
	WT OE	3.47 ± 1.35 (0.590)	2.93 ± 1.21 (0.673)	2.73 ± 1.59 (0.761)
	S81L OE	4.27 ± 0.723 (0.150)	3.20 ± 0.730 (0.407)	5.00 ± 2.12 (0.265)
Retrograde Flux				
	Control	2.40 ± 1.38	2.13 ± 1.66	3.67 ± 2.16
	WT OE	3.00 ± 1.63 (0.796)	2.47 ± 1.63 (0.903)	2.27 ± 1.48 (0.375)
	S81L OE	2.93 ± 1.94 (0.834)	1.60 ± 0.683 (0.776)	3.27 ± 1.55 (0.911)

3.2.2. Percentage of Total Mitochondrial Movement

Male Percentage of Total Mitochondrial Movement

The majority of mitochondria within an axon are stationary, with a small percentage showing anterograde movement, and an even smaller percentage showing retrograde movement. All averages, standard deviations, and p-values are provided in Table 5. There were no statistically significant differences in the percentage of mitochondrial movement between the groups and across expression lines in male larvae, indicating there were similar rates of movement (Figure 9 A, B, C; Table 5).

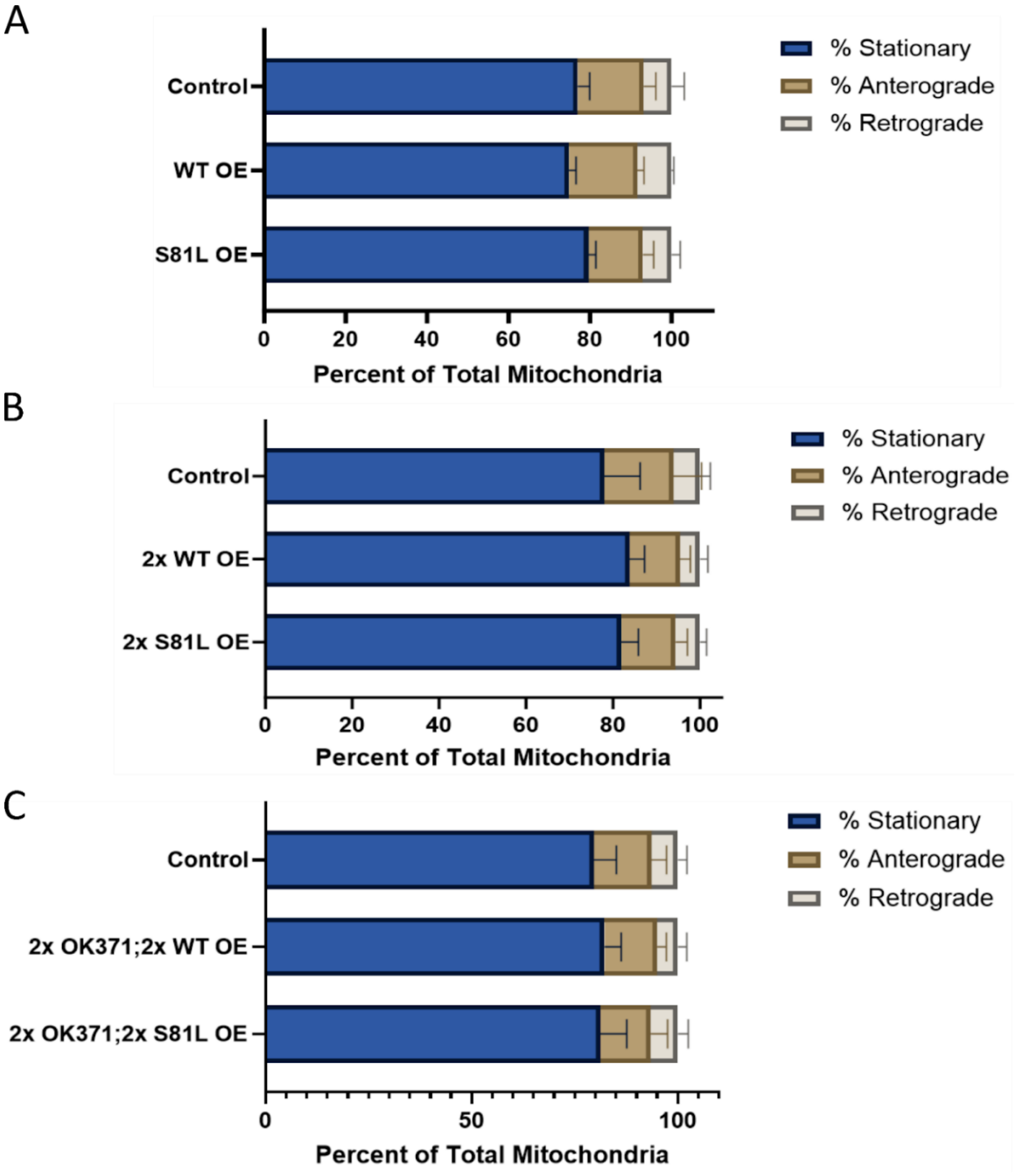

Figure 9: Percentage of total mitochondrial movement in male larvae. (A) Percentage of mitochondrial movement in heterozygous males. **(B)** Percentage of mitochondrial movement in homozygous males. **(C)** Percentage of mitochondrial movement in double homozygous males. Data are shown as mean ± SD.

Table 5: Male percentage of total mitochondrial movement averages ± standard deviation (p-value).

Parameter	Experimental Group	Heterozygous	Homozygous	Double Homozygous
% Stationary				
	Control	77.0 ± 2.92	78.0 ± 8.25	79.6 ± 5.50
	WT OE	74.8 ± 1.97 (0.301)	83.8 ± 3.42 (0.248)	82.2 ± 4.09 (0.733)
	S81L OE	79.6 ± 1.82 (0.199)	81.8 ± 4.02 (0.554)	81.2 ± 6.38 (0.887)
% Anterograde				
	Control	16.2 ± 2.95	15.8 ± 6.57	14.0 ± 3.67
	WT OE	16.8 ± 1.64 (0.922)	11.6 ± 2.41 (0.311)	12.8 ± 2.17 (0.845)
	S81L OE	13.4 ± 2.61 (0.212)	12.6 ± 2.70 (0.493)	12.2 ± 4.09 (0.690)
% Retrograde				
	Control	6.80 ± 3.11	6.20 ± 2.39	6.40 ± 2.19
	WT OE	8.40 ± 0.548 (0.503)	4.60 ± 1.82 (0.420)	5.00 ± 2.12 (0.608)
	S81L OE	7.00 ± 2.12 (0.989)	5.60 ± 1.52 (0.878)	6.60 ± 2.51 (0.990)

Female Percentage of Total Mitochondrial Movement

All averages, standard deviations, and p-values are provided in Table 6. Similar to males, there were no statistically significant differences in the percentage of mitochondrial movement between the groups and across expression lines in female larvae, again meaning there were similar rates of movement (Figure 10 A, B, C; Table 6).

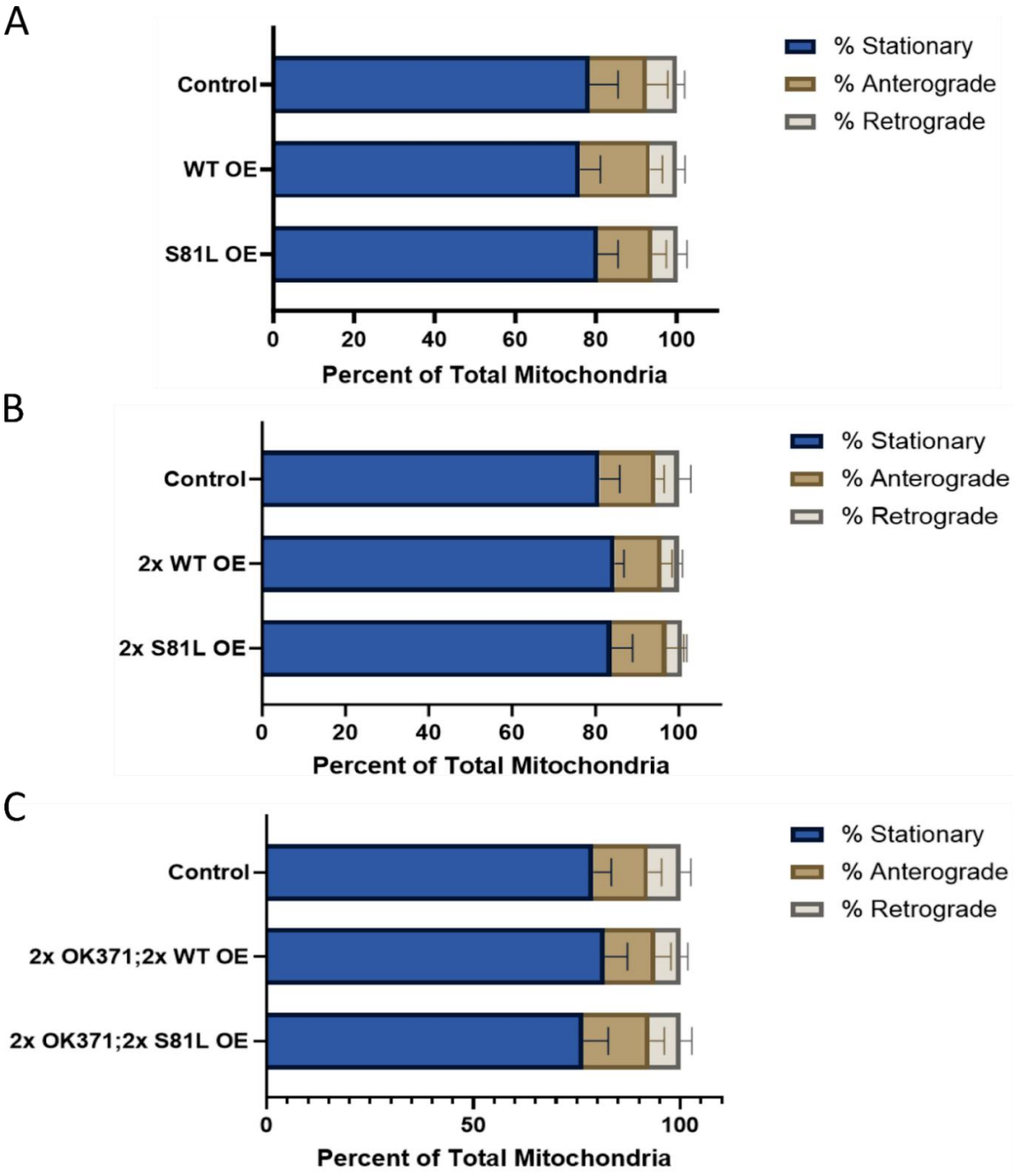

Figure 10: Percentage of total mitochondrial movement in female larvae. (A) Percentage of mitochondrial movement in heterozygous females. **(B)** Percentage of mitochondrial movement in homozygous females. **(C)** Percentage of mitochondrial movement in double homozygous females. Data are shown as mean ± SD.

Table 6: Female percentage of total mitochondrial movement averages ± standard deviation (p-value).

Parameter	Experimental Group	Heterozygous	Homozygous	Double Homozygous
% Stationary				
	Control	78.4 ± 7.09	81.0 ± 4.85	79.0 ± 4.30
	WT OE	76.0 ± 5.05 (0.795)	84.6 ± 2.19 (0.400)	81.8 ± 5.45 (0.688)
	S81L OE	80.4 ± 5.08 (0.852)	83.8 ± 5.07 (0.565)	76.6 ± 5.98 (0.758)
% Anterograde				
	Control	14.2 ± 5.22	13.4 ± 2.07	13.2 ± 3.27
	WT OE	17.4 ± 3.05 (0.442)	11.2 ± 2.59 (0.512)	12.2 ± 3.77 (0.896)
	S81L OE	13.6 ± 3.44 (0.970)	13.2 ± 4.15 (0.994)	16.0 ± 3.54 (0.446)
% Retrograde				
	Control	7.40 ± 1.95	5.60 ± 2.88	7.80 ± 2.59
	WT OE	6.60 ± 2.07 (0.828)	4.20 ± 0.837 (0.475)	6.00 ± 1.87 (0.497)
	S81L OE	6.20 ± 2.39 (0.660)	3.80 ± 1.10 (0.306)	7.40 ± 2.79 (0.964)

3.2.3. Velocity

Male Velocity

All velocity averages, standard deviations, and p-values are provided in Table 7. Male heterozygous WT anterograde mitochondria had an average velocity of 0.289 μm/sec and control mitochondria had an average velocity of 0.217 μm/sec. Therefore, as expected, heterozygous WT mitochondria exhibited significantly faster anterograde velocities (Figure 11 A; Table 7). Similarly, homozygous WT anterograde mitochondria had an average velocity of 0.202 μm/sec and the control had an average velocity of 0.166 μm/sec, thus homozygous WT mitochondria also displayed significantly faster velocities compared to the control in the anterograde direction (Figure 11 B; Table 7). Double homozygous WT male anterograde mitochondria had an average velocity of 0.170 μm/sec while the control average velocity was 0.207 μm/sec. Thus, unexpectedly, double

homozygous WT mitochondria displayed significantly slower velocities in the anterograde direction (Figure 11 C; Table 7).

2x S81L male mitochondria trended towards faster velocities in the anterograde direction compared to the control, but it was not statistically significant ($p = 0.0884$, AES: 0.0249) (Figure 11 B; Table 7). Double homozygous WT retrograde mitochondria trended towards slower average velocities compared to the control, but not significantly ($p = 0.0512$, AES: 0.104) (Figure 11 F; Table 7). 1x S81L and double homozygous S81L expression did not produce any significant differences in anterograde velocities compared to the control (Figure 11 A, C; Table 7). For retrograde velocities, there were no significant differences between 1x S81L, 1x WT, 2x S81L, 2x WT, and double homozygous S81L and the control (Figure 11 D, E, F; Table 7).

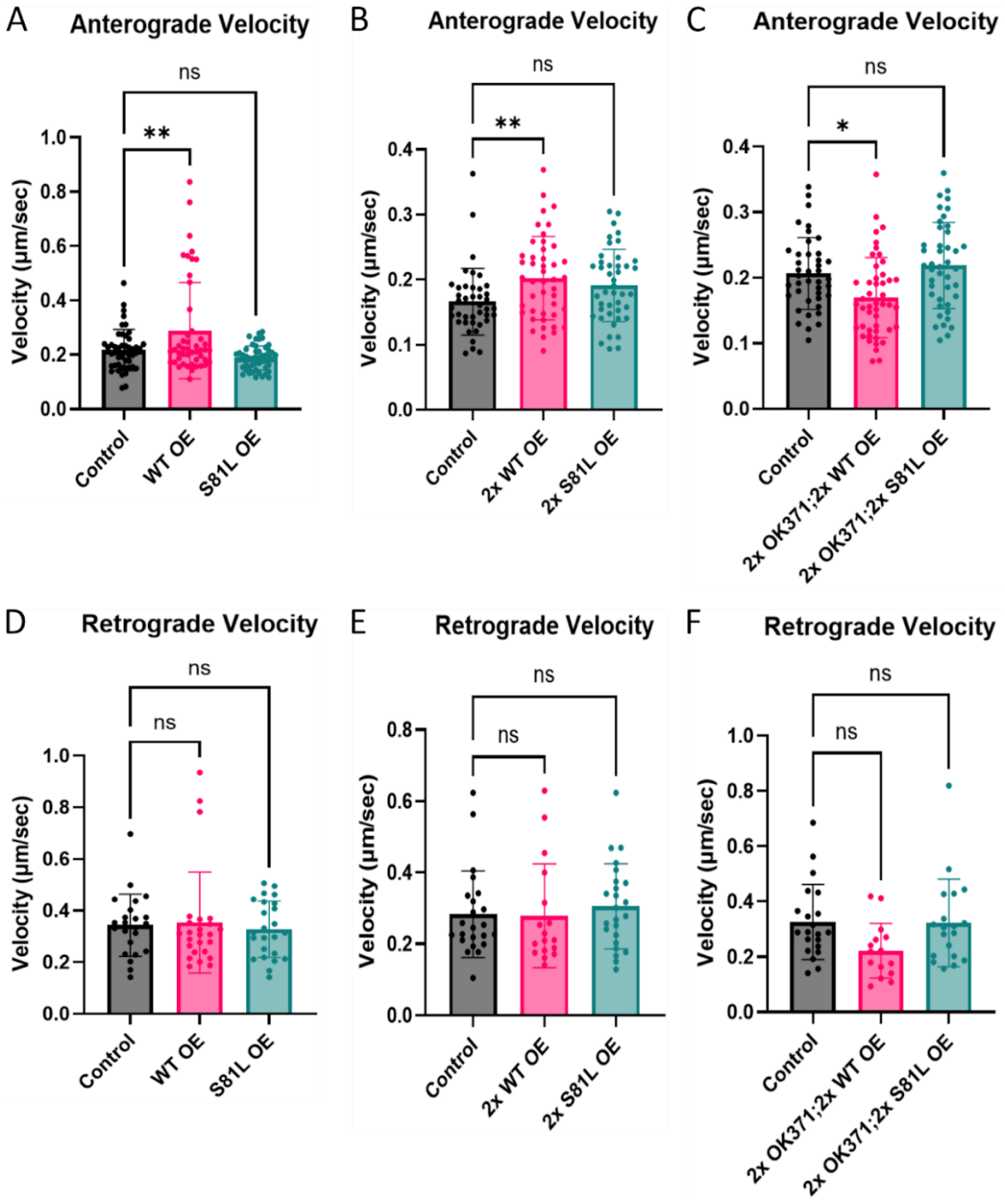

Figure 11: Velocity in male larvae. (A) Quantification of anterograde velocity for heterozygous males. **(B)** Quantification of anterograde velocity for homozygous males. **(C)** Quantification of anterograde velocity for double homozygous males. **(D)** Quantification of retrograde velocity for heterozygous males. **(E)** Quantification of retrograde velocity for homozygous males. **(F)** Quantification of retrograde velocity for double homozygous males. Data are shown as mean ± SD. NS: not significant. * $p < 0.05$. ** $p < 0.01$.

Table 7: Male velocity averages ± standard deviation (p-value).

Parameter	Experimental Group	Heterozygous	Homozygous	Double Homozygous
Anterograde Velocity				
	Control	0.217 ± 0.076	0.166 ± 0.051	0.207 ± 0.055
	WT OE	0.289 ± 0.177 (0.005)	0.202 ± 0.064 (0.008)	0.170 ± 0.061 (0.010)
	S81L OE	0.188 ± 0.044 (0.344)	0.191 ± 0.056 (0.088)	0.219 ± 0.066 (0.558)
Retrograde Velocity				
	Control	0.344 ± 0.120	0.283 ± 0.121	0.326 ± 0.136
	WT OE	0.354 ± 0.196 (0.958)	0.279 ± 0.145 (0.992)	0.222 ± 0.099 (0.051)
	S81L OE	0.328 ± 0.109 (0.911)	0.306 ± 0.119 (0.774)	0.323 ± 0.158 (0.997)

Female Velocity

All velocity averages, standard deviations, and p-values are provided in Table 8. Heterozygous WT anterograde mitochondria had an average velocity of 0.208 μm/sec while the control average was 0.162 μm/sec, thus 1 copy of WT in females led to significantly faster velocities in the anterograde direction compared to the control (Figure 12 A; Table 8). Heterozygous WT mitochondria also displayed significantly faster velocities in the retrograde direction, with an average velocity of 0.346 μm/sec for WT mitochondria and 0.233 μm/sec for control mitochondria (Figure 12 D; Table 8). Homozygous S81L mitochondria exhibited significantly faster velocities than the control in the anterograde direction with an average velocity of 0.193 μm/sec for S81L mitochondria and 0.162 μm/sec for control mitochondria (Figure 12 B; Table 8). Double homozygous WT mitochondria had significantly slower velocities in both anterograde and retrograde directions compared to the control (Figure 12 C, F; Table 8). The average

velocity of anterograde mitochondria was 0.187 μm/sec for double homozygous WT females and 0.234 μm/sec for the control. The average velocity of retrograde mitochondria was 0.292 μm/sec for double homozygous WT females and 0.403 μm/sec for the control.

Contrary to our expectations, 1x S81L mitochondria trended towards faster velocities in the retrograde direction compared to the control, although the difference was not statistically significant ($p = 0.102$, AES: 0.0580) (Figure 12 D; Table 8). Double homozygous S81L mitochondria trended towards slower velocities in the anterograde direction compared to the control, but it was not significant ($p = 0.0716$, AES: 0.0301) (Figure 12 C; Table 8). 1x S81L and 2x WT did not produce significantly different velocities of anterograde mitochondria compared to the control (Figure 12 A, C; Table 8). 2x S81L, 2x WT, and double homozygous S81L expression also did not produce statistically significant differences in retrograde velocities compared to the control (Figure 8 E, F; Table 8).

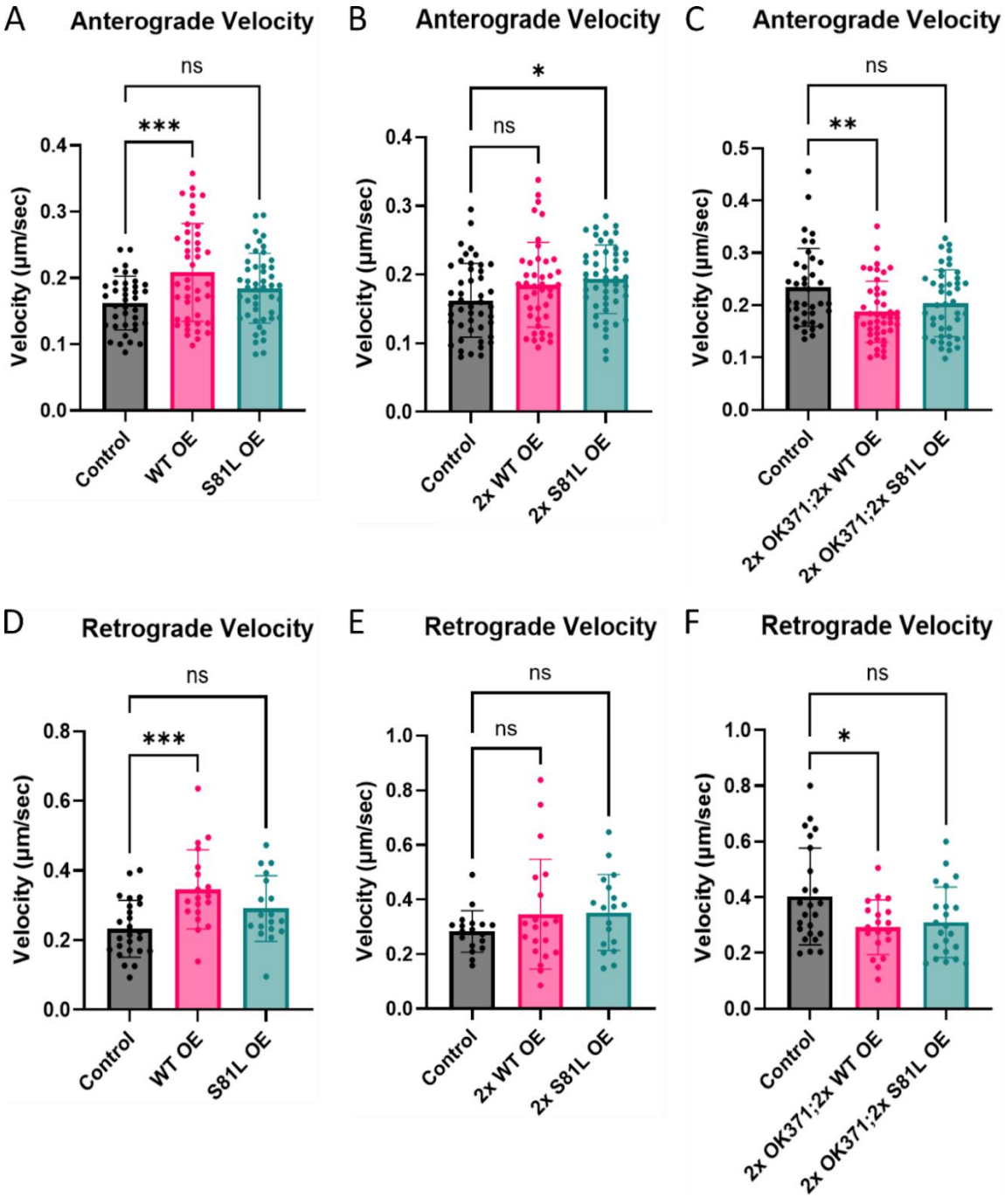

Figure 12: Velocity in female larvae. (A) Quantification of anterograde velocity for heterozygous females. **(B)** Quantification of anterograde velocity for homozygous females. **(C)** Quantification of anterograde velocity for double homozygous females. **(D)** Quantification of retrograde velocity for heterozygous females. **(E)** Quantification of retrograde velocity for homozygous females. **(F)** Quantification of retrograde velocity for double homozygous females. Data are shown as mean ± SD. NS: not significant. * $p < 0.05$. ** $p < 0.01$. *** $p < 0.001$.

Table 8: Female velocity averages ± standard deviation (p-value).

Parameter	Experimental Group	Heterozygous	Homozygous	Double Homozygous
Anterograde Velocity				
	Control	0.162 ± 0.041	0.162 ± 0.054	0.234 ± 0.074
	WT OE	0.208 ± 0.074 (0.001)	0.185 ± 0.062 (0.100)	0.187 ± 0.059 (0.003)
	S81L OE	0.185 ± 0.053 (0.134)	0.193 ± 0.050 (0.013)	0.204 ± 0.064 (0.072)
Retrograde Velocity				
	Control	0.233 ± 0.082	0.283 ± 0.076	0.403 ± 0.174
	WT OE	0.346 ± 0.114 (0.0005)	0.346 ± 0.201 (0.328)	0.292 ± 0.098 (0.023)
	S81L OE	0.291 ± 0.094 (0.102)	0.352 ± 0.139 (0.285)	0.310 ± 0.127 (0.513)

3.2.4. Distance

Male Distance

All distance averages, standard deviations, and p-values are provided in Table 9. Heterozygous S81L male anterograde mitochondria traveled an average distance of 20.7 μm while control anterograde mitochondria traveled an average distance of 25.1 μm. Therefore, 1 copy of S81L in males led to mitochondria traveling significantly shorter distances in the anterograde direction compared to the control (Figure 13 A; Table 9). Heterozygous WT anterograde mitochondria traveled an average distance of 19.7 μm, thus 1 copy of WT in males led mitochondria to also travel significantly shorter distances in the anterograde direction compared to the control (Figure 13 A; Table 9). Double homozygous WT expression in males led mitochondria to travel significantly shorter distances compared to the control in the retrograde direction as double homozygous WT

retrograde mitochondria traveled an average distance of 20.0 μm while the control mitochondria traveled an average distance of 32.0 μm (Figure 13 F; Table 9).

For anterograde distance, 2x S81L and WT, and double homozygous S81L and WT did not produce significant differences compared to the control (Figure 13 B, C; Table 9). Expression of 1x S81L and WT, 2x S81L and WT, and double homozygous S81L also did not produce significant differences in retrograde distances compared to the control (Figure 13 D, E, F; Table 9).

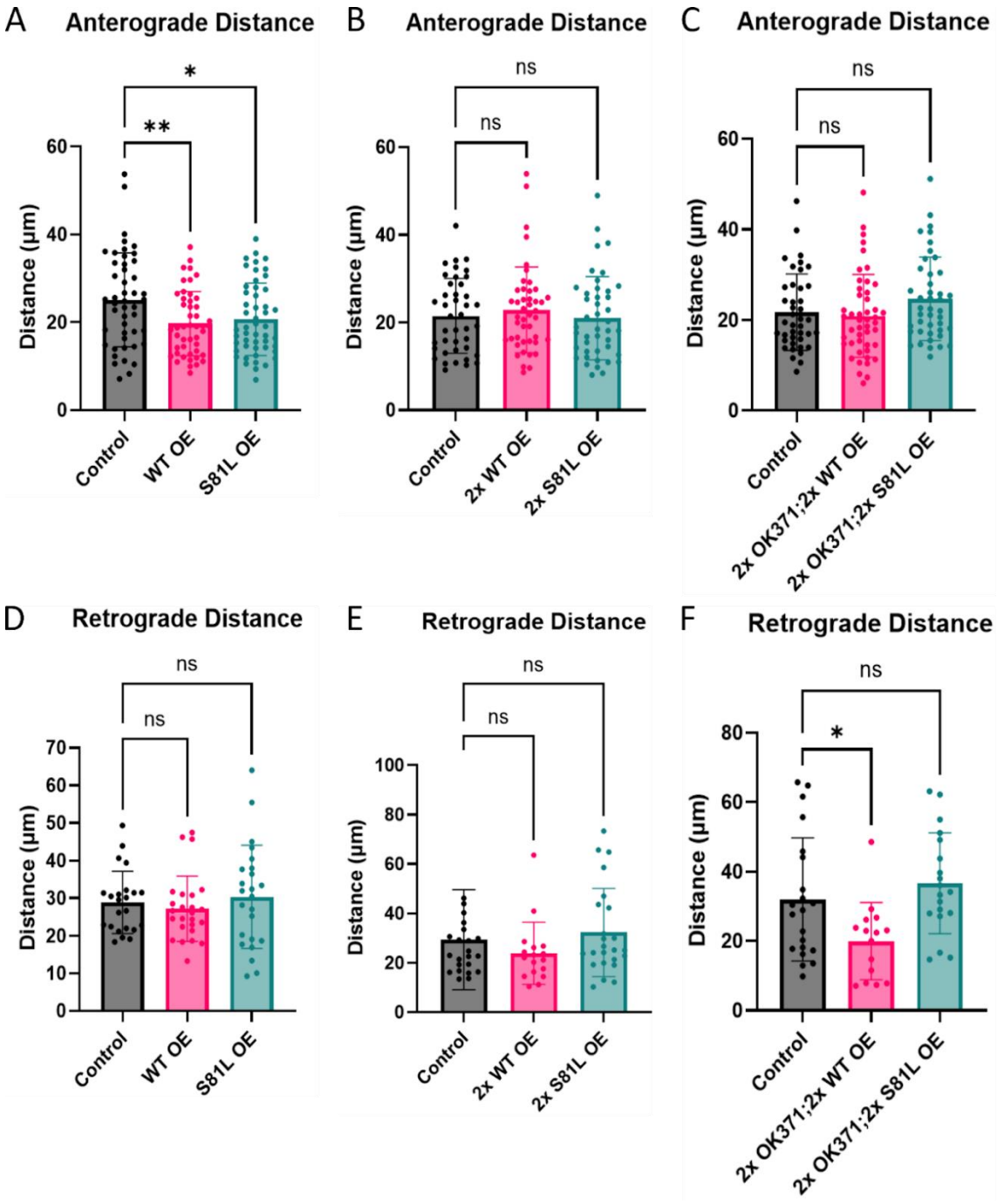

Figure 13: Distance in male larvae. (A) Quantification of anterograde distance for heterozygous males. **(B)** Quantification of anterograde distance for homozygous males. **(C)** Quantification of anterograde distance for double homozygous males. **(D)** Quantification of retrograde distance for heterozygous males. **(E)** Quantification of retrograde distance for homozygous males. **(F)** Quantification of retrograde distance for double homozygous males. Data are shown as mean ± SD. NS: not significant. * $p < 0.05$. ** $p < 0.01$.

Table 9: Male distance averages ± standard deviation (p-value).

Parameter	Experimental Group	Heterozygous	Homozygous	Double Homozygous
Anterograde Distance				
	Control	25.1 ± 10.7	21.5 ± 8.52	21.7 ± 8.41
	WT OE	19.7 ± 7.31 (0.007)	22.9 ± 9.80 (0.702)	20.9 ± 9.16 (0.873)
	S81L OE	20.7 ± 8.25 (0.028)	21.0 ± 9.48 (0.956)	24.7 ± 9.24 (0.228)
Retrograde Distance				
	Control	28.8 ± 8.29	29.4 ± 20.3	32.0 ± 17.8
	WT OE	27.2 ± 8.67 (0.800)	23.9 ± 12.6 (0.521)	20.0 ± 11.2 (0.042)
	S81L OE	30.3 ± 13.7 (0.844)	32.3 ± 17.8 (0.805)	36.6 ± 14.5 (0.535)

Female Distance

All distance averages, standard deviations, and p-values are provided in Table 10. Overall, there were no statistically significant differences in distance traveled, however, 2x S81L anterograde mitochondria traveled an average distance of 25.3 μm while the control traveled an average of 17.1 μm. Therefore, 2 copies of S81L in females led to mitochondria traveling significantly further distances compared to the control in the anterograde direction (Figure 14 B; Table 10).

As expected, 1x WT mitochondria trended towards traveling further distances than the control in the anterograde direction, but not significantly further ($p = 0.0723$, AES: 3.84) (Figure 14 A; Table 10). 2x S81L mitochondria also trended towards traveling further than the control in the retrograde direction, but again, not significantly further ($p = 0.107$, AES: 10.8) (Figure 14 E; Table 10). Unexpectedly, double homozygous WT mitochondria trended towards traveling shorter distances compared to the control in the anterograde direction ($p = 0.0526$, AES: 4.39) (Figure 14 C; Table 10). 1x S81L, 2x WT, and double homozygous S81L mitochondria did not display significant

differences in anterograde distance compared to the control (Figure 14 A, B, C; Table 10). For retrograde distance, there were no significant differences between 1x S81L, 1x WT, 2x WT, double homozygous S81L, and double homozygous WT and the control (Figure 14 D, E, F; Table 10).

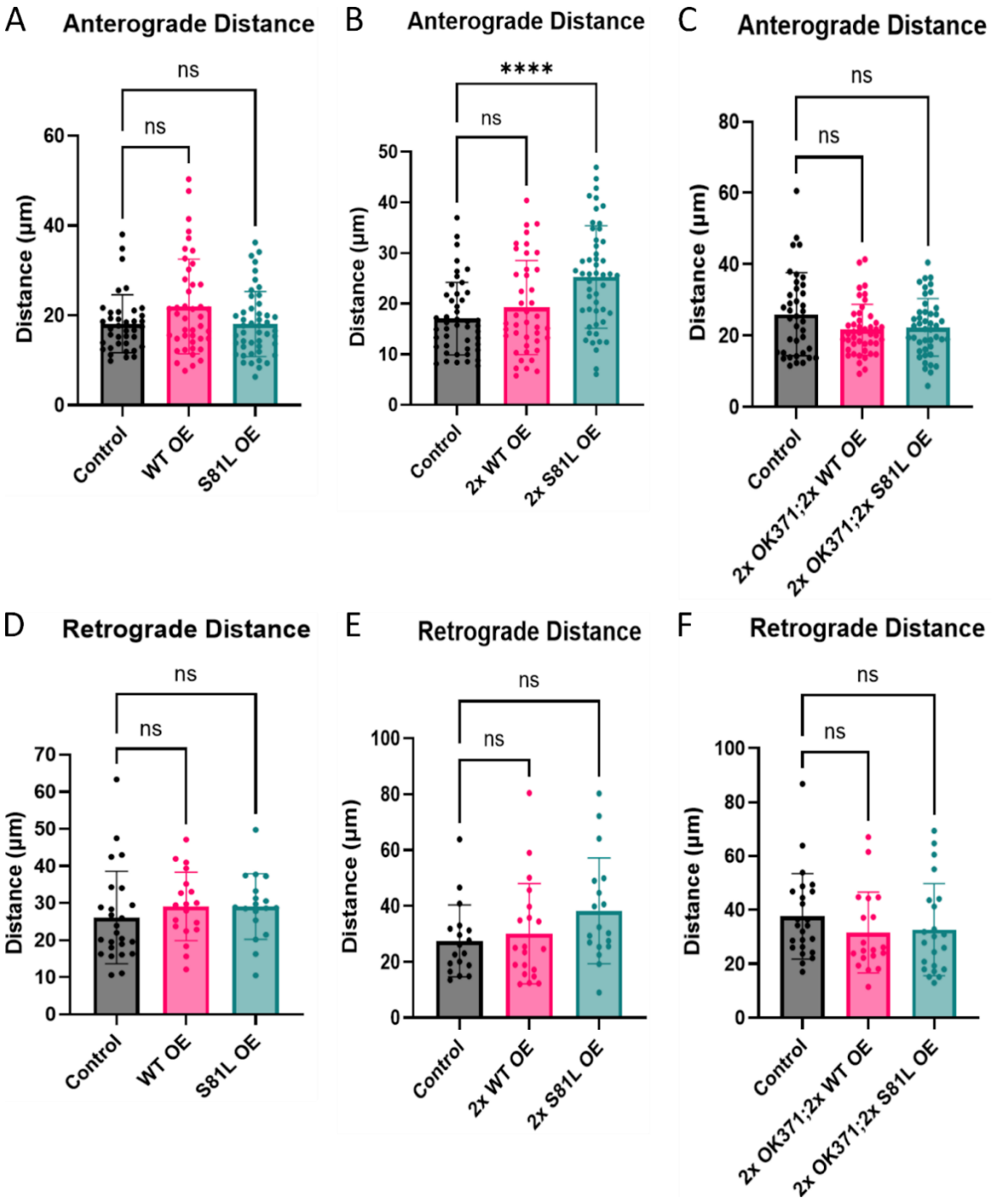

Figure 14: Distance in female larvae. (A) Quantification of anterograde distance for heterozygous females. **(B)** Quantification of anterograde distance for homozygous females. **(C)** Quantification of anterograde distance for double homozygous females. **(D)** Quantification of retrograde distance for heterozygous females. **(E)** Quantification of retrograde distance for homozygous females. **(F)** Quantification of retrograde distance for double homozygous females. Data are shown as mean ± SD. NS: not significant. **** $p < 0.0001$.

Table 10: Female distance averages ± standard deviation (p-value).

Parameter	Experimental Group	Heterozygous	Homozygous	Double Homozygous
Anterograde Distance				
	Control	18.13 ± 6.44	17.1 ± 7.15	26.0 ± 11.7
	WT OE	22.0 ± 10.6 (0.072)	19.2 ± 9.28 (0.423)	21.6 ± 7.16 (0.053)
	S81L OE	18.08 ± 7.25 (0.9995)	25.3 ± 10.1 (0.00005)	22.3 ± 8.05 (0.117)
Retrograde Distance				
	Control	26.1 ± 12.4	27.5 ± 12.9	37.6 ± 15.8
	WT OE	29.1 ± 9.22 (0.559)	30.1 ± 17.9 (0.853)	31.6 ± 15.0 (0.377)
	S81L OE	29.0 ± 8.84 (0.575)	38.3 ± 18.9 (0.107)	32.7 ± 17.1 (0.485)

3.2.5. Run Length

Male Run Length

Run length measures the persistence of transport. Longer run lengths mean that the mitochondrion likely stopped less often, whereas a shorter run length means that the mitochondrion likely stopped more often. All run length averages, standard deviations, and p-values are provided in Table 11. Heterozygous S81L male anterograde mitochondria had an average run length of 2.39 μm while the control average was 3.18 μm, therefore, expression of 1 copy of S81L in males led anterograde mitochondria to have significantly shorter run lengths compared to the control (Figure 15 A; Table 11). Unexpectedly, heterozygous WT male mitochondria also displayed significantly shorter run lengths in the anterograde direction compared to the control as heterozygous WT anterograde mitochondria had an average run length of 2.54 μm (Figure 15 A, Table 11).

Double homozygous WT male mitochondria trended towards shorter run lengths compared to the control in the retrograde direction, but it was not statistically significant ($p = 0.0555$, AES: 1.75) (Figure 15 F; Table 11). Expression of 2x S81L, 2x WT, double

homozygous S81L, and double homozygous WT did not produce significant differences in anterograde run length compared to the control (Figure 15 B, C; Table 11). There were no significant differences in retrograde run length between the control and 1x S81L, 1x WT, 2x S81L, 2x WT, and double homozygous S81L groups (Figure 15 D, E, F; Table 11).

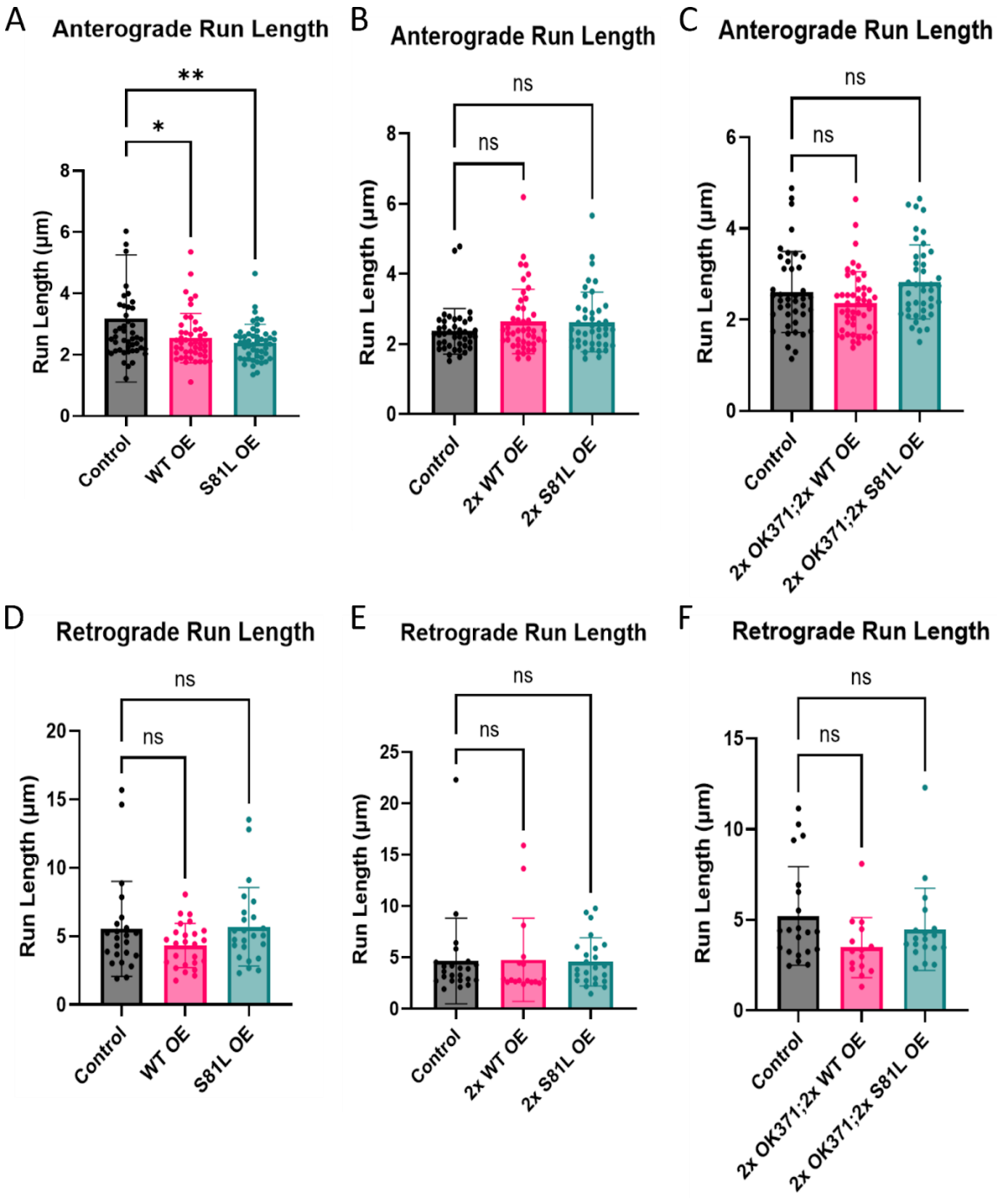

Figure 15: Run length in male larvae. (A) Quantification of anterograde run length for heterozygous males. **(B)** Quantification of anterograde run length for homozygous males. **(C)** Quantification of anterograde run length for double homozygous males. **(D)** Quantification of retrograde run length for heterozygous males. **(E)** Quantification of retrograde run length for homozygous males. **(F)** Quantification of retrograde run length for double homozygous males. Data are shown as mean ± SD. NS: not significant. * $p < 0.05$. ** $p < 0.01$.

Table 11: Male run length averages ± standard deviation (p-value).

Parameter	Experimental Group	Heterozygous	Homozygous	Double Homozygous
Anterograde Run Length				
	Control	3.18 ± 2.07	2.36 ± 0.649	2.61 ± 0.890
	WT OE	2.54 ± 0.808 (0.038)	2.64 ± 0.923 (0.194)	2.37 ± 0.688 (0.262)
	S81L OE	2.39 ± 0.594 (0.007)	2.63 ± 0.849 (0.238)	2.83 ± 0.814 (0.341)
Retrograde Run Length				
	Control	5.54 ± 3.47	4.65 ± 4.17	5.22 ± 2.71
	WT OE	4.32 ± 1.62 (0.220)	4.77 ± 4.05 (0.992)	3.48 ± 1.66 (0.056)
	S81L OE	5.69 ± 2.87 (0.972)	4.57 ± 2.35 (0.996)	4.48 ± 2.26 (0.505)

Female Run Length

All run length averages, standard deviations, and p-values are provided in Table 12. Heterozygous WT female anterograde mitochondria had an average run length of 2.73 μm while the average for the control was 2.19 μm. 1x WT female retrograde mitochondria had an average run length of 4.64 μm and the control average was 3.47 μm. Thus, 1 copy of WT in females led to significantly longer run lengths in both directions compared to the control (Figure 16 A, D; Table 12). Double homozygous S81L mitochondria exhibited significantly shorter run lengths compared to the control in the retrograde direction as double homozygous S81L retrograde had an average run length of 4.49 μm while the control average was 7.26 μm (Figure 16 F; Table 12). Similarly, double homozygous WT mitochondria exhibited significantly shorter run lengths in the retrograde direction as double homozygous WT retrograde mitochondria had an average run length of 4.64 um (Figure 16 F; Table 12). 1x S81L, 2x S81L, 2x WT, double homozygous S81L, and double homozygous WT expression did not produce statistically significant differences in anterograde run length compared to the control (Figure 16 A, B,

C; Table 12). For retrograde run length, there were no significant differences between 1x S81L, 2x S81L, and 2x WT and the control (Figure 16 D, E, F; Table 12).

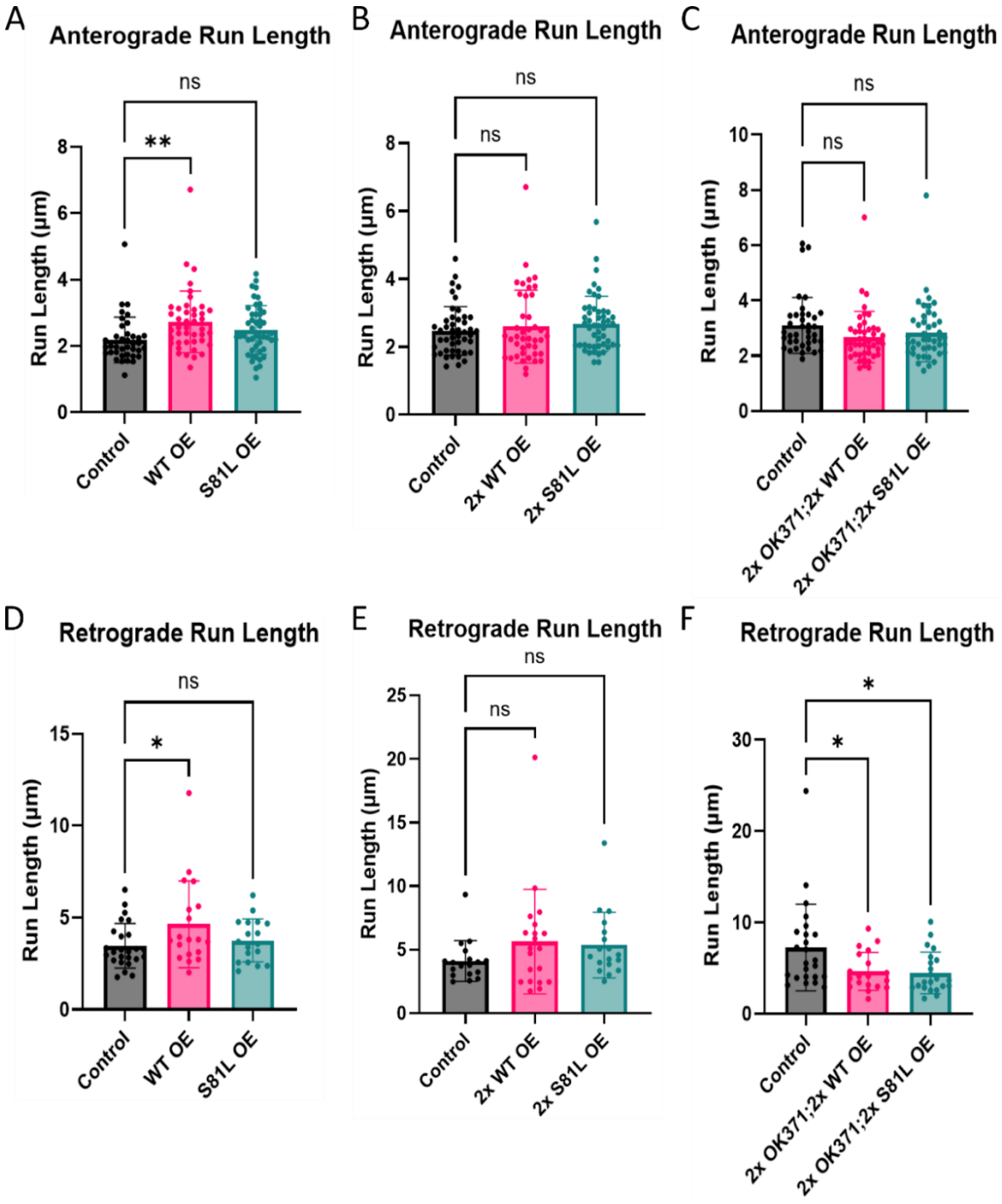

Figure 16: Run length in female larvae. (A) Quantification of anterograde run length for heterozygous females. **(B)** Quantification of anterograde run length for homozygous females. **(C)** Quantification of anterograde run length for double homozygous females. **(D)** Quantification of retrograde run length for heterozygous females. **(E)** Quantification of retrograde run length for homozygous females. **(F)** Quantification of retrograde run length for double homozygous females. Data are shown as mean ± SD. NS: not significant. * $p < 0.05$. ** $p < 0.01$

Table 12: Female run length averages ± standard deviation (p-value).

Parameter	Experimental Group	Heterozygous	Homozygous	Double Homozygous
Anterograde Run Length				
	Control	2.19 ± 0.687	2.47 ± 0.715	3.10 ± 1.01
	WT OE	2.73 ± 0.928 (0.005)	2.59 ± 1.07 (0.728)	2.68 ± 0.925 (0.101)
	S81L OE	2.48 ± 0.733 (0.151)	2.68 ± 0.811 (0.399)	2.84 ± 1.05 (0.380)
Retrograde Run Length				
	Control	3.47 ± 1.21	4.11 ± 1.59	7.26 ± 4.75
	WT OE	4.64 ± 2.35 (0.042)	5.63 ± 4.10 (0.212)	4.64 ± 2.09 (0.027)
	S81L OE	3.76 ± 1.17 (0.795)	5.36 ± 2.58 (0.352)	4.49 ± 2.27 (0.014)

3.2.6. Duty Cycle

Male Duty Cycle

Duty cycle describes the percentage of time a single mitochondrion spends either stationary, moving in the anterograde direction, or moving in the retrograde direction. Net anterograde mitochondria spend the majority of their time moving in the anterograde direction, a smaller percentage of time being stationary, and an even smaller percentage of time reversing direction to move in the retrograde direction. Conversely, net retrograde mitochondria spend the majority of their time moving in the retrograde direction, a small percentage of time being stationary, and an even smaller percentage of time reversing to move in the anterograde direction.

Averages, standard deviations, and p-values of anterograde duty cycle are provided in Table 13 and averages, standard deviations, and p-values of retrograde duty cycle are provided in Table 14. Homozygous WT net anterograde mitochondria spent an average time of 10.8% being stationary, while control mitochondria spent an average time of 20.1% being stationary. Thus 2 copies of WT in males led net anterograde

mitochondria to spend significantly less time in the stationary phase compared to the control (Figure 17 B; Table 13). Consequently, homozygous WT net anterograde mitochondria spent an average time of 81.4% moving in the anterograde direction, while control mitochondria spent only 74.1% of their time moving in the anterograde direction. Thus, 2 copies of WT in males led net anterograde mitochondria to spend significantly more time moving in the anterograde direction compared to the control (Figure 17 B; Table 13).

Double homozygous WT net anterograde mitochondria spent an average time of 18.6% being stationary, while control mitochondria spent an average time of 12.0% in the stationary phase. Thus, double homozygous WT expression in males led net anterograde mitochondria to spend significantly more time in the stationary phase compared to the control (Figure 17 C; Table 13). As a result, double homozygous WT net anterograde mitochondria spent an average time of 72.9% moving in the anterograde direction, while the control mitochondria spent 80.9% of their time moving in the anterograde direction. Therefore, double homozygous WT net anterograde mitochondria spent significantly less time moving in the anterograde direction compared to the control (Figure 17 C; Table 13). Double homozygous WT net retrograde mitochondria also spent an average time of 22.2% being stationary while the control average was 13.9%, thus double homozygous WT expression in males led to net retrograde mitochondria to spend significantly more time being stationary compared to the control (Figure 17 C; Table 14). Consequently, double homozygous WT net retrograde mitochondria spent an average time of 63.7% moving in the retrograde direction while the control average was 75.6%, therefore double

homozygous WT expression in males led net retrograde mitochondria to spend significantly less time moving in the retrograde direction compared to the control (Figure 17 C; Table 14).

Double homozygous S81L net retrograde mitochondria trended towards spending more time reversing to move in the anterograde direction compared to the control ($p = 0.0884$, AES: 4.16) (Figure 17 F; Table 14). Conversely, double homozygous S81L net retrograde mitochondria trended towards spending less time moving in the retrograde direction compared to the control ($p = 0.1992$, AES: 6.70) (Figure 17 F; Table 14). There were no statistically significant differences in anterograde or retrograde duty cycles of heterozygous S81L and WT mitochondria in males compared to the control (Figure 17 A, D; Table 13, Table 14). There were no significant differences in anterograde and retrograde duty cycles for homozygous S81L males compared to the control (Figure 17 B, E; Table 13, Table 14). Additionally, there were no significant differences in retrograde duty cycles for homozygous WT mitochondria (Figure 17 E; Table 14). Double homozygous S81L expression in males did not result in statistically significant differences in anterograde duty cycles, as well as percentage of time spent stationary for net retrograde mitochondria (Figure 17 C, F; Table 13, Table 14). There were no significant differences in the percentage of time spent reversing to move in the retrograde direction for net anterograde mitochondria between the control and 2x WT and double homozygous WT groups (Figure 17 B, C; Table 13). Further, double homozygous WT expression did not produce significant differences in the percentage of time spent reversing to the anterograde direction of net retrograde mitochondria compared to the

control (Figure 18 F; Table 14).

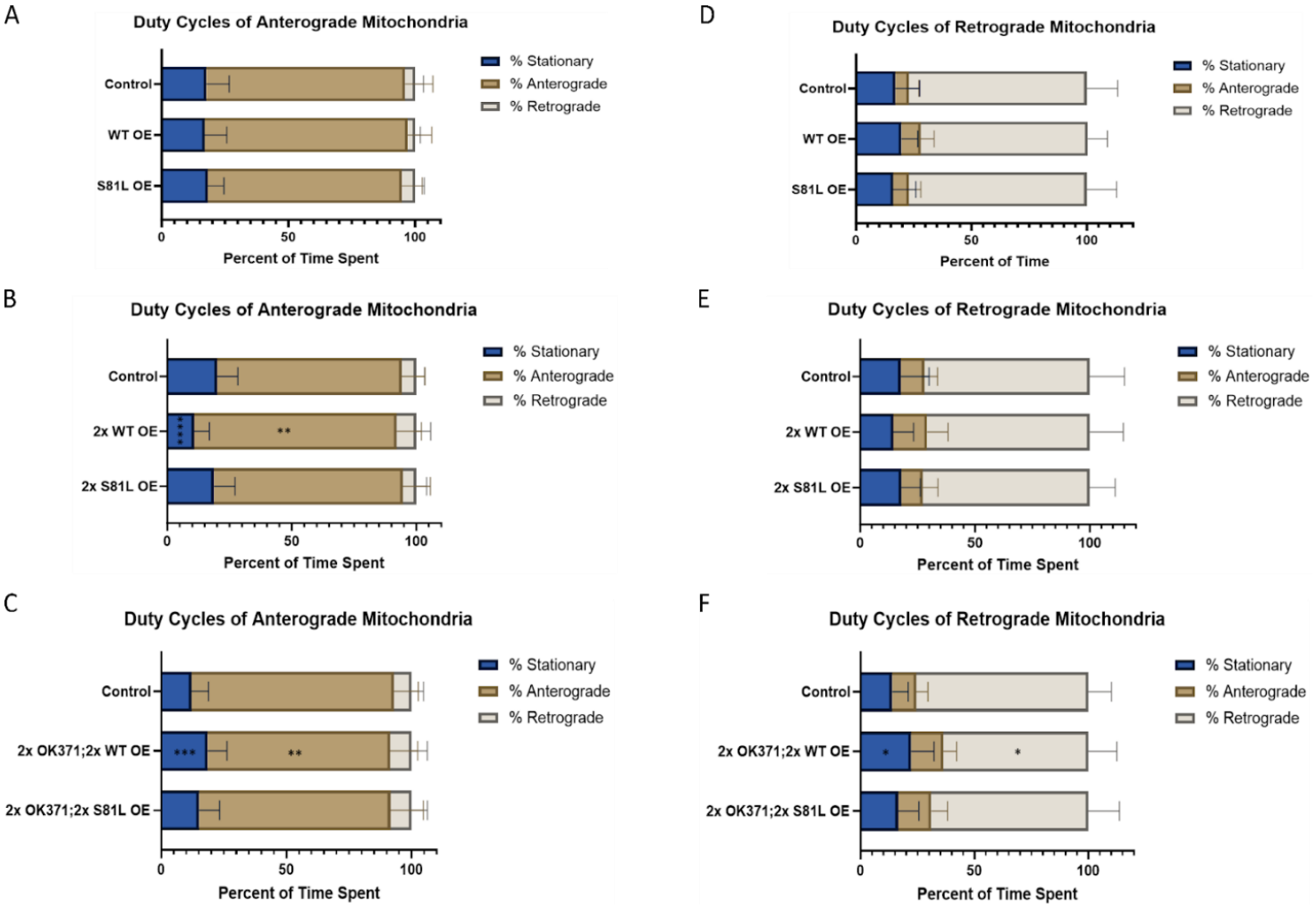

Figure 17: Duty cycles in male larvae. (A) Quantification of anterograde duty cycles for heterozygous males. **(B)** Quantification of anterograde duty cycles for homozygous males. **(C)** Quantification of anterograde duty cycles for double homozygous males. **(D)** Quantification of retrograde duty cycles for heterozygous males. **(E)** Quantification of retrograde run duty cycles for homozygous males. **(F)** Quantification of retrograde duty cycles for double homozygous males. Data are shown as mean ± SD. NS: not significant. * $p < 0.05$. ** $p < 0.01$. *** $p < 0.001$. **** $p < 0.0001$.

Table 13: Male anterograde duty cycle averages ± standard deviation (p-value).

Parameter	Experimental Group	Heterozygous	Homozygous	Double Homozygous
% of Time Stationary				
	Control	17.7 ± 8.95	20.1 ± 8.28	12.0 ± 6.82
	WT OE	17.0 ± 8.76 (0.907)	10.8 ± 6.15 (0.0000004)	18.6 ± 7.69 (0.0003)
	S81L OE	18.2 ± 6.38 (0.953)	18.8 ± 8.47 (0.733)	15.1 ± 8.19 (0.160)
% of Time Anterograde				
	Control	78.3 ± 11.0	74.1 ± 9.32	80.9 ± 9.73
	WT OE	80.0 ± 9.59 (0.690)	81.4 ± 9.86 (0.003)	72.9 ± 11.0 (0.003)
	S81L OE	76.6 ± 8.10 (0.647)	75.8 ± 11.1 (0.730)	76.5 ± 13.1 (0.172)
% of Time Retrograde				
	Control	3.99 ± 3.33	5.85 ± 3.29	7.01 ± 4.80
	WT OE	3.06 ± 2.07 (0.319)	7.81 ± 5.74 (0.118)	8.55 ± 6.27 (0.443)
	S81L OE	5.24 ± 3.64 (0.119)	5.46 ± 4.14 (0.920)	8.43 ± 6.34 (0.514)

Table 14: Male retrograde duty cycle averages ± standard deviation (p-value).

Parameter	Experimental Group	Heterozygous	Homozygous	Double Homozygous
% of Time Stationary				
	Control	17.1 ± 10.5	17.7 ± 12.3	13.9 ± 7.03
	WT OE	19.7 ± 7.03 (0.589)	14.5 ± 8.69 (0.586)	22.2 ± 10.0 (0.018)
	S81L OE	16.0 ± 9.88 (0.919)	18.0 ± 8.18 (0.994)	16.5 ± 9.10 (0.624)
% of Time Anterograde				
	Control	5.80 ± 4.37	10.3 ± 5.70	10.5 ± 5.17
	WT OE	8.34 ± 5.82 (0.211)	14.6 ± 9.08 (0.148)	14.1 ± 5.83 (0.185)
	S81L OE	6.90 ± 5.12 (0.746)	9.16 ± 6.66 (0.844)	14.6 ± 7.14 (0.088)
% of Time Retrograde				
	Control	77.1 ± 13.4	72.0 ± 15.1	75.6 ± 10.2
	WT OE	72.0 ± 8.58 (0.291)	70.9 ± 14.6 (0.963)	63.7 ± 12.6 (0.014)
	S81L OE	77.07 ± 13.0 (0.999)	72.9 ± 11.1 (0.975)	68.9 ± 13.7 (0.199)

Female Duty Cycle

Averages, standard deviations, and p-values for anterograde duty cycle are provided in Table 15 and averages, standard deviations, and p-values for retrograde duty cycle are provided in Table 16. Homozygous S81L net anterograde mitochondria spent an average time of 12.8% being stationary while the control average was 18.2%. Thus, 2 copies of S81L in females resulted in net anterograde mitochondria spending significantly less time in the stationary phase compared to the control (Figure 18 B; Table 15). Additionally, homozygous S81L net retrograde mitochondria spent an average time of 14.7% reversing to move in the anterograde direction while the control average was 9.13%. Therefore, homozygous S81L net retrograde mitochondria spent significantly more time reversing to the anterograde direction compared to the control (Figure 18 E; Table 16). Homozygous WT net anterograde mitochondria spent an average time of 12.8% being stationary while the control spent an average time of 18.2% being stationary. Thus, homozygous WT net anterograde mitochondria spent significantly less time being stationary compared to the control (Figure 18 B; Table 15). Consequently, homozygous WT net anterograde mitochondria spent an average time of 9.77% reversing to the retrograde direction, while the control average was 5.09%. Thus, 2x WT expression in females led net anterograde mitochondria to spend significantly more time reversing to the retrograde direction compared to the control (Figure 18 B; Table 15).

Double homozygous S81L net anterograde mitochondria spent an average time of 9.89% reversing to move in the retrograde direction, while the control average was 6.89%, therefore double homozygous S81L expression in females led net anterograde

mitochondria to spend a significantly higher percentage of time reversing to the retrograde direction (Figure 18 C; Table 15). Double homozygous S81L net retrograde mitochondria spent an average time of 16.5% reversing to the anterograde direction, while the control average was 9.83%. Therefore, double homozygous S81L expression in females led net retrograde mitochondria to spent significantly more time reversing to the anterograde direction (Figure 18 F; Table 16).

Double homozygous S81L net anterograde mitochondria trended towards spending less time moving in the anterograde direction compared to the control ($p = 0.0931$, AES: 4.77) (Figure 18 C; Table 15). Double homozygous S81L net retrograde mitochondria trended towards spending less time moving in the retrograde direction compared to the control ($p = 0.1492$, AES: 6.58) (Figure 18 F; Table 16). Double homozygous WT net retrograde mitochondria also trended towards spending less time moving in the retrograde direction compared to the control ($p = 0.269$, AES: 5.66) (Figure 18 F; Table 16). Like heterozygous male duty cycles, there were no statistically significant differences in anterograde or retrograde duty cycles of heterozygous S81L and WT mitochondria in females (Figure 18 A, D; Table 15, Table 16). Expression of double homozygous S81L did not produce significant differences in percentage of time spent stationary for net anterograde mitochondria compared to the control (Figure 18 C; Table 15). There were no significant differences in percentage of time spent moving in the anterograde direction for net anterograde mitochondria between 2x S81L and the control (Figure 18 B; Table 14). 2x S81L net anterograde mitochondria did not exhibit a significant difference in percentage of time spent reversing to move in the retrograde

direction compared to the control (Figure 18 B; Table 15). For net retrograde mitochondria percentage of time spent stationary, there were no significant differences between 2x S81L and double homozygous S81L and the control (Figure 18 E, F; Table 16). Expression of 2x S81L did not produce a significant difference in net retrograde mitochondria for percentage of time spent moving in the retrograde direction compared to the control (Figure 18 E; Table 16). There were no significant differences in retrograde duty cycle between 2x WT and the control (Figure 18 E; Table 16). Further, there were no significant differences in anterograde duty cycle of double homozygous WT expression in females (Figure 18 C; Table 15). Double homozygous WT net retrograde mitochondria also did not display a significant difference in percentage of time spent in the stationary phase and percentage of time spent reversing to move in the anterograde direction compared to the control (Figure 18 F; Table 16).

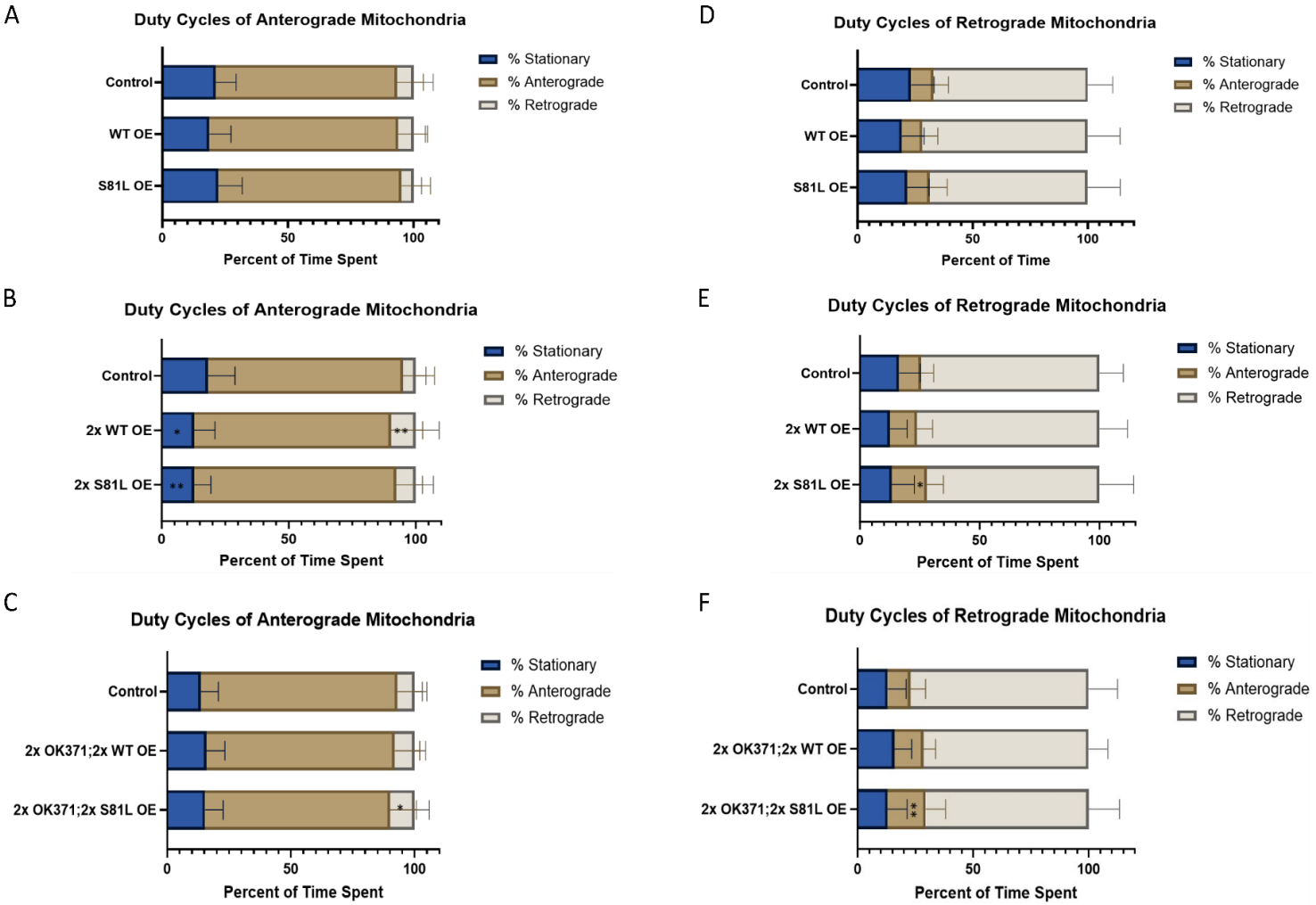

Figure 18: Duty cycles in female larvae. (A) Quantification of anterograde duty cycles for heterozygous females. **(B)** Quantification of anterograde duty cycles for homozygous females. **(C)** Quantification of anterograde duty cycles for double homozygous females. **(D)** Quantification of retrograde duty cycles for heterozygous females. **(E)** Quantification of retrograde run duty cycles for homozygous females. **(F)** Quantification of retrograde duty cycles for double homozygous females. Data are shown as mean ± SD. NS: not significant. * $p < 0.05$. ** $p < 0.01$.

Table 15: Female anterograde duty cycle averages ± standard deviation (p-value).

Parameter	Experimental Group	Heterozygous	Homozygous	Double Homozygous
% of Time Stationary				
	Control	21.2 ± 8.21	18.2 ± 10.7	13.5 ± 7.17
	WT OE	18.7 ± 8.59 (0.434)	12.8 ± 8.20 (0.010)	15.9 ± 7.46 (0.311)
	S81L OE	22.2 ± 9.59 (0.852)	12.8 ± 6.54 (0.007)	15.3 ± 7.30 (0.518)
% of Time Anterograde				
	Control	72.2 ± 10.5	76.7 ± 12.4	79.6 ± 10.0
	WT OE	75.1 ± 11.8 (0.498)	77.4 ± 12.5 (0.952)	76.1 ± 10.1 (0.278)
	S81L OE	73.0 ± 11.5 (0.943)	79.4 ± 10.4 (0.488)	74.8 ± 10.6 (0.093)
% of Time Retrograde				
	Control	6.60 ± 7.81	5.09 ± 3.95	6.89 ± 4.98
	WT OE	6.20 ± 4.71 (0.940)	9.77 ± 9.17 (0.005)	7.99 ± 4.46 (0.598)
	S81L OE	4.75 ± 3.21 (0.263)	7.76 ± 6.90 (0.145)	9.89 ± 5.95 (0.027)

Table 16: Female retrograde duty cycle averages ± standard deviation (p-value).

Parameter	Experimental Group	Heterozygous	Homozygous	Double Homozygous
% of Time Stationary				
	Control	23.3 ± 9.99	16.4 ± 8.87	13.0 ± 7.91
	WT OE	19.3 ± 9.60 (0.379)	12.5 ± 7.20 (0.355)	15.9 ± 7.42 (0.463)
	S81L OE	21.5 ± 9.66 (0.820)	13.3 ± 9.46 (0.521)	12.95 ± 8.41 (0.999)
% of Time Anterograde				
	Control	9.74 ± 6.42	9.13 ± 5.26	9.83 ± 6.50
	WT OE	8.73 ± 6.78 (0.880)	11.2 ± 6.52 (0.560)	12.6 ± 5.18 (0.409)
	S81L OE	9.86 ± 7.63 (0.998)	14.7 ± 6.95 (0.029)	16.5 ± 8.62 (0.006)
% of Time Retrograde				
	Control	67.0 ± 10.9	74.5 ± 9.95	77.1 ± 12.5
	WT OE	72.0 ± 14.0 (0.413)	76.2 ± 11.7 (0.900)	71.5 ± 8.29 (0.269)
	S81L OE	68.7 ± 14.1 (0.904)	72.1 ± 14.3 (0.820)	70.6 ± 13.4 (0.149)

4. Discussion and Concluding Remarks

Mitochondrial transport is needed to maintain cellular health. In the case of neurons, mitochondrial transport is required to get the organelles to where they are needed, such as synapses, to help mediate synaptic communication. Reduced mitochondrial transport is seen in many neurodegenerative disease models, including other ALS disease mutations, suggesting inadequate mitochondrial motility may contribute to the pathogenesis of such neurodegenerative diseases. The ALS-FTD-causing mutation CHCHD10^{S59L} causes mitochondrial dysfunction leading to abnormal mitochondrial morphology and function. Thus, the goal of the present study was to determine if neurons expressing the S59L mutation had abnormal mitochondrial transport as well. We expected to see a decrease in mitochondrial motility in S59L neurons compared to the control. Due to the goal of this study, most of the discussion will focus on differences between control expression and S59L expression.

While the expression of CHCHD10^{S59L} in flies (C2C10H^{S81L}) did lead to abnormal mitochondrial motility, the results were not as we expected, and they were not seen across the board. There are a total of 6 transport parameters that were analyzed using three distinct expression lines, while also analyzing males and females separately. This results in 36 separate outcomes (102 when taking direction and stationary phases into account). Of the 36, only 10 produced a statistically significant difference between the control group and the S81L group (Figure 19; Table 17; Table 18). Heterozygous S81L male mitochondria displayed significantly less anterograde movement, significantly shorter distances traveled of anterograde mitochondria, and significantly shorter run

lengths of anterograde mitochondria compared to the control (Figure 7 A, D; Figure 13 A; Figure 15 A). Homozygous S81L expression in females led anterograde mitochondria to display significantly faster velocities, to travel significantly further distances, and to spend significantly less time being stationary (Figure 12 B; Figure 14 B; Figure 18 B). Additionally, 2x S81L female retrograde mitochondria spent significantly more time reversing direction to move in the anterograde direction compared to the control (Figure 18 E). Double homozygous S81L female anterograde mitochondria spent significantly more time reversing to travel in the retrograde direction (Figure 18 C). Further, double homozygous S81L female retrograde mitochondria has significantly shorter run lengths and spent significantly more time reversing direction to move in the anterograde direction compared to the control (Figure 15 F; Figure 18 F).

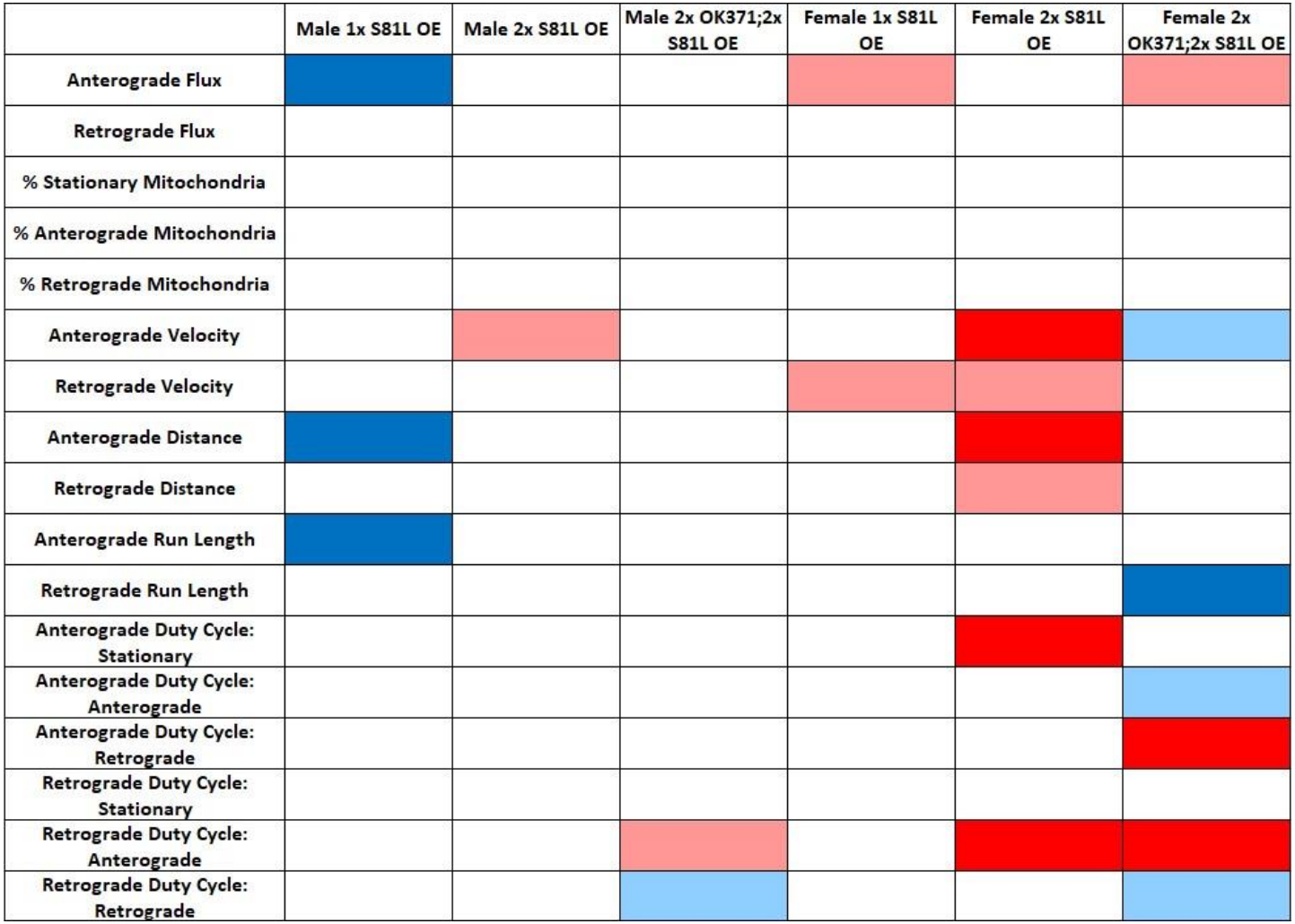

Figure 19: A summary heat map for mitochondrial motility in S81L flies of all the parameters, taking direction into account. Red color indicates a statistically significant increase in mitochondrial motility compared to the control. Pink color indicated that parameter showed a trend for increased motility compared to the control. Blue color indicates a statistically significant decrease in mitochondrial motility compared to the control. Light blue color indicates that parameter showed a trend for decreased motility compared to the control. White boxes indicate there was no statistical significance.

Table 17: Summary table of statistical significance for mitochondrial transport in male S81L flies compared to their respective control genotype. The last row is the trend S81L mitochondria exhibit compared to the control when considering statistically significant data (dark colored boxes in Figure 19) and trends of statistically significant data (light colored boxed in Figure 19). NS: nonsignificant.

	Heterozygous	**Homozygous**	**Double Homozygous**
Flux	Less anterograde transport	NS	NS
Percent Mitochondrial Movement	NS	NS	NS
Velocity	NS	NS	NS
Distance	Shorter in the anterograde direction	NS	NS
Run Length	Shorter in the anterograde direction	NS	NS
Duty Cycle	NS	NS	NS
Overall Movement Trend Compared to Control	Reduced	Increased	Indeterminable

Table 18: Summary table of statistical significance for mitochondrial transport in female S81L flies compared to their respective control genotype. The last row is the trend S81L mitochondria exhibit compared to the control when considering statistically significant data (dark colored boxes in Figure 19) and trends of statistically significant data (light colored boxed in Figure 19). NS: nonsignificant. AS: net Anterograde mitochondria that are Stationary. RA: net Retrograde mitochondria reversing to move in the Anterograde direction. AR: net Anterograde mitochondria reversing to move in the Retrograde direction.

	Heterozygous	**Homozygous**	**Double Homozygous**
Flux	NS	NS	NS
Percent Mitochondrial Movement	NS	NS	NS
Velocity	NS	Faster in the anterograde direction	NS
Distance	NS	Longer in the anterograde direction	NS
Run Length	NS	NS	Shorter in the retrograde direction
Duty Cycle	NS	Less AS. More RA	More AR. More RA
Overall Movement Trend Compared to Control	Increased	Increased	Reduced

Even though only 10 out of the 36 outcomes produced statistically significant data, there were several trends present. An overall trend is that mitochondria displayed an overall bias for more or less mitochondrial transport. For instance, 1 copy of S81L expression in males led to overall less movement. This is supported by the fact that male S81L mitochondria exhibited statistically less anterograde flux, shorter distances, and shorter run lengths (Figure 19).While some of the other parameters saw a statistically nonsignificant increase in motility, male heterozygous S81L mitochondria showed a trend for reduced movement compared to the control, which is what we expected (Table 17). Conversely, female heterozygous S81L mitochondria displayed overall more movement. Female 1x S81L mitochondria trended towards higher rates of anterograde flux and faster retrograde velocities (Figure 19). Similar to heterozygous males, some of the parameters displayed a statistically nonsignificant decrease in motility, but overall, female heterozygous S81L mitochondria showed a trend for increased transport compared to the control, which is not what we expected (Table 18).

Homozygous expression of S81L in males resulted in overall increased mitochondrial transport. 2x S81L anterograde mitochondria exhibited trends of faster anterograde velocities (Figure 19). Similar to the heterozygous models, there were some parameters that had decreased transport, but overall, male homozygous S81L mitochondria trended towards more mitochondrial transport compared to the control (Table 17). This was unexpected as we anticipated the homozygous model having a more severe phenotype compared to the heterozygous model, therefore, we were expecting to see a decrease in mitochondrial transport beyond that of the heterozygous S81L male

model. Similarly, female homozygous S81L mitochondria also displayed more movement. 2x S81L mitochondria exhibited significantly faster anterograde velocities, significantly further anterograde distance, significantly less time spent in the stationary phase for anterograde duty cycle, and significantly more time moving in the anterograde direction for retrograde duty cycle (Figure 19). 2x S81L female mitochondria also displayed trends for faster retrograde velocities and longer retrograde distances (Figure 19). Thus, female homozygous S81L mitochondria trended towards more mitochondrial transport compared to the control (Table 18). Even though we expected decreased motility in S81L neurons, we technically did see a more severe phenotype in the homozygous female model compared to the heterozygous female model. Some parameters that were not statistically significant in the heterozygous model became statistically significant in the homozygous model, thus the female homozygous model displayed even more motility than the heterozygous model, indicating a dose-dependent response.

The overall bias for increased or decreased motility was also present in the WT models. As expected, female heterozygous and homozygous WT models, and the male homozygous WT model, led to more mitochondrial movement compared to the control (Supplementary Figure 1; Supplementary Table 1, Supplementary Table 2). 1x WT expression in females led mitochondria to exhibit significantly faster velocities and significantly longer run lengths, while also showing a trend for longer anterograde distances (Supplementary Figure 1). 2x WT in males had mitochondria exhibit significantly faster anterograde velocities, and significantly more movement in

anterograde duty cycles, while also displaying a trend for increased anterograde movement in retrograde duty cycles (Supplementary Figure 1). Likewise, 2x WT in females led mitochondria to exhibit significantly more movement in anterograde duty cycles and display a trend for longer retrograde run lengths (Supplementary Figure 1). Thus, female heterozygous and homozygous WT mitochondria, and male homozygous WT mitochondria trended towards more mitochondrial transport compared to the control, which again, is consistent with our expectation (Supplementary Table 1; Supplementary Table 2). 1x WT mitochondria exhibited significantly faster anterograde velocities, but significantly shorter anterograde distances and run lengths while also displaying a trend for decreased anterograde flux, shorter retrograde run lengths, and less retrograde movement in retrograde duty cycles (Supplementary Figure 1). Thus, even though 1x WT mitochondria displayed increased movement in some parameters, the overall bias was a trend for decreased mitochondrial transport (Supplementary Table 1).

Double homozygous expression of WT or S81L in males and females resulted in a trend of decreased mitochondrial transport, except for double homozygous S81L males which didn't show an overall bias for increased or decreased transport compared to the control (Table 17; Table 18; Supplementary Table 1; Supplementary Table 2). The number of parameters showing a trend for decreased motility compared to increased motility for double homozygous S81L females was 4:3, while there was no difference in double homozygous S81L males (1 decreased: 1 increased) (Figure 19). Similar to the above paragraph, these numbers reflect the movement behavior of statistically significant data and trends of statistically nonsignificant data. Interestingly, expression of double

homozygous WT in both males and females resulted in little to no parameters showing a trend for increased motility (8 decreased: 1 increased for males; 5 decreased: 0 increased for females). This likely suggests too much expression of WT is not beneficial and may disrupt normal function. A direct comparison between the heterozygous and homozygous models and the double homozygous model could not be made because the double homozygous model carries 2 copies of OK371, and thus has a different genetic background compared to the heterozygous and homozygous models.

Likely the biggest trend was the increase in motility of S81L mitochondria when going from the heterozygous model to the homozygous model. In males, 1 copy of S81L led mitochondria to have significantly less movement than the control. Upon 2 copies of S81L, this parameter (flux) became nonsignificant, meaning there was an increase in motility. This was also seen in females. 1 copy of S81L did not produce statistically significant differences, but expression of 2 copies of S81L resulted in significantly faster anterograde velocities, again showing an increase in motility. This trend is also seen even when the data was not statistically significant. For example, female heterozygous S81L retrograde mitochondria had an average velocity of 0.291 μm/sec, while homozygous S81L retrograde mitochondria had an average velocity of 0.353 μm/sec. This increase in motility when going from the heterozygous model to the homozygous model can also be seen in other transport parameters such as both directions of distance and anterograde run lengths in males and females.

In summary, genotypes that displayed a trend for less mitochondrial transport were heterozygous S81L males, double homozygous S81L females, heterozygous WT

males, and double homozygous WT males and females, while the genotypes that displayed a trend for increased mitochondrial transport were homozygous S81L males, heterozygous S81L females, homozygous S81L females, homozygous WT males, heterozygous WT females, and homozygous WT females (Figure 19; Table 18; Table 19; Supplementary Figure 1; Supplementary Table 1; Supplementary Table 2). Double homozygous S81L males showed an indeterminable trend for motility compared to the control (Figure 19; Table 18). Additionally, there was an increase in mitochondrial transport when going from 1x S81L to 2x S81L expression.

One reason that could explain this inconsistent data between males and females and between different expression lines is that larvae are actively developing, and mitochondria play many roles in this development. While larvae generally use aerobic glycolysis for their development, mitochondria are still needed for metabolism during the growth process (Tennessen et al., 2011). The TCA cycle takes place inside the mitochondria, and the TCA cycle is the primary source of protein, lipid, and amino acid precursors (Jacobs et al., 2020). This suggests that mitochondria are greatly needed during larval development to help convert monomers into macromolecules. Additionally, mitochondria have their own genome and disruptions in its transcription and eventual translation lead to increased levels of apoptosis in developing larvae, ultimately leading to lethality (Adán et al., 2008). Moreover, differentiation and proliferation of larval neural stem cells require mitochondrial respiration and its calcium buffering capacity (Tiwari and Mandal, 2021). Furthermore, developing larvae are actively making more neurons, more dendrites, and more axonal branches, all of which are very energy-

demanding processes and require ATP. In fact, rates of neurogenesis for adult-specific neurons are highest during the larval stage (Truman and Riddiford, 2023). Developing axons, or growth cones, extend via lamellipodia and filopodia which is mediated by dynamic changes in actin filaments (Smith and Gallo, 2018). These dynamic changes require ATP to add actin monomers to the existing filament chain, and it is estimated that up to 50% of cellular ATP generated by mitochondria are used to continually extend the growth cone (Bernstein and Bamburg, 2003). Pioneering studies demonstrated that mitochondria accumulate in the central domain of the growth cone and mitochondria are continually transported in the anterograde direction as the axon extends (Morris and Hollenbeck, 1993; Ruthel and Hollenbeck, 2003). Further, when an axonal branch does not undergo extension, mitochondria are retrogradely transported and moved to a more proximal axonal branch that is undergoing extension (Smith and Gallo, 2018). Together, this suggests that mitochondria likely play a multitude of roles in larval development.

The growth and development of larvae could also explain the rates of anterograde transport compared to retrograde transport. Across all expression lines, there were more data points for anterograde mitochondria than retrograde mitochondria. This was not intentional, as there were truly fewer mitochondria moving in the retrograde direction compared to the anterograde direction. This bias towards anterograde transport also supports the notion that mitochondria are needed distally for axon elongation (Frederick and Shaw, 2007), as stated in the previous paragraph. Additionally, net retrograde mitochondria spent more time reversing direction to move in the anterograde direction compared to net anterograde mitochondria reversing to move in the retrograde direction.

This parameter (duty cycle) was seen across genotypes and expression lines, especially in females. Thus, it's likely that there was more anterograde movement than retrograde movement because more mitochondria are needed distally to aid in larval growth and development.

Taken together, this rather inconsistent data could suggest growth effects and/or an unknown compensation mechanism may be at play, and any mitochondrial transport defects that could be present in S81L larvae are outweighed by the need for increased mitochondrial motility to support their growth and development. A potential compensation mechanism can be seen in the increased motility of S81L mitochondria when going from a heterozygous model to a homozygous model. As previously mentioned, one copy of S81L in males led to statistically significant reduced mitochondrial transport in anterograde flux, distance, and run length. Upon homozygous expression, these parameters became nonsignificant, meaning there was an increase in motility from the heterozygous model to the homozygous model. In S81L females, one copy of S81L did not lead to any statistically significant data. However, with two copies of S81L, anterograde mitochondria displayed statistically significant faster velocities and longer distances. Thus, again, there was an increase in motility when going from the heterozygous model to the homozygous model.

One way to address this inconsistent data would be to repeat this entire project in the adult fruit fly system. Ultimately, the adult fly system was not used in the present study due to the methodology and time constraints. However, with appropriate timing and practice, the method for analyzing mitochondrial transport in adult fly wings could

become robust. The present study would have benefited from the adult system as it is a truly aged model and thus is more representative of the ALS-FTD population. If adult S81L flies exhibited decreased mitochondrial transport, then it is likely that the lack of significance overall in the present study and increased motility of S81L larvae could truly be due to them actively growing and needing the increased mitochondrial transport to support that growth. If there is not a reduction in adult S81L flies, then it is likely that mitochondrial transport has little or no impact on the pathogenesis of CHCHD10^{S59L}-mediated ALS-FTD.

Another pertinent future direction would be to evaluate the effects PINK1 has on mitochondrial transport in an S81L model. PINK1 is a kinase and plays an important role in the PINK1/Parkin pathway. This pathway is responsible for degrading damaged mitochondria and halting mitochondrial transport. In a healthy mitochondrion, PINK1 is translocated into the mitochondrion where it is cleaved and degraded. However, upon mitochondrial damage, PINK1 accumulates on the outer mitochondrial membrane (OMM) surface. PINK1 then phosphorylates preexisting ubiquitin chains, as well as the ubiquitin-like domain of Parkin, an E3 ubiquitin ligase. Phosphorylation of Parkin causes its activation and accumulation on the OMM surface, leading to polyubiquitination of OMM proteins by Parkin (Li et al., 2023). These OMM proteins are then degraded by the proteasome. Removing the OMM proteins blocks the function of the mitochondrion, thus allowing it to get degraded. Similarly, PINK1 halts anterograde mitochondrial transport by phosphorylating MIRO, part of the motor/adaptor complex used to transport mitochondria in the anterograde direction. Parkin then causes the degradation of MIRO,

breaking the connection between the motor adaptor complex and the microtubule, resulting in mitochondrial arrest (Wang et al., 2011). Interestingly, overexpression of PINK1 resulted in mitochondrial arrest in both anterograde and retrograde directions (Wang et al., 2011), suggesting that mitochondrial transport is PINK1-dependent in both anterograde and retrograde directions.

In our 2021 study showing mitochondrial dysfunction occurs in CHCHD10^{S59L} cells, we also observed that PINK1 significantly accumulated on mitochondria in this specific mutation (Baek et al., 2021). Upon knockdown of PINK1, cells with the S59L mutation exhibited rescued mitochondrial morphology and respiration, suggesting that the accumulation of PINK1 on mitochondria is toxic to the cells (Baek et al., 2021). At the beginning of the present study, PINK1-dependent transport was supposed to be included. If S81L mitochondria had displayed reduced transport in the larval system, PINK1 RNAi lines would have been utilized to determine the effect of knocking down PINK1 had on mitochondrial transport. Based on previous literature and our findings that PINK1 accumulates in this disease model, we would expect to see a rescue of mitochondrial motility in S81L flies that co-expressed PINK1 RNAi. However, due to the inconsistent data and the overall trend of S81L mitochondria showing increased motility, possibly due to growth effects or unknown potential compensation mechanisms, PINK1 was not included in the present study. Thus, this future direction in the adult model system would help further elucidate the role PINK1-dependent mitochondrial transport has in the pathogenesis of CHCHD10^{S59L}-mediated ALS-FTD.

Another very useful future direction would be to add an *in vitro* model. The present study attempted to use differentiated SH-SY5Y cells to evaluate mitochondrial transport in an *in vitro* system. However, consistent differentiation was a problem, and due to time constraints, further troubleshooting was not performed. SH-SY5Y cells were chosen over other cells because of their mature neuron-like phenotype when differentiated, and culturing of this cell line is less expensive and requires less skill than some other cells lines like induced pluripotent stem cells (iPSCs). Therefore, troubleshooting SH-SY5Y differentiation until consistent differentiation is achieved, or using iPSCs, would allow an *in vitro* model to be used for investigating mitochondrial transport in CHCHD10^{S59L}-mediated ALS-FTD. The present study would have greatly benefited from a successful *in vitro* model, as it likely could have shed some light into the inconsistent data gathered in the larval system, and also would have helped determine if these S81L larvae really do have increased motility because of their active development.

If adult S81L flies exhibit decreased mitochondrial transport, another future experiment would be to quantify the transport machinery. Quantifying proteins such as kinesin, MIRO, TRAK, dynein, dynactin, and SNHP could help determine if the reduced transport is due to a reduction in the transport machinery, or if another mechanism is at play. In several neurodegenerative disease models, the respective toxic protein can interact with mitochondria directly, resulting in reduced transport (Devine and Kittler, 2018), while another study showed that the mutant SOD1 protein in ALS interacts with the transport machinery and disrupts mitochondrial motility that way (Moller et al., 2017). Furthermore, it would be interesting to see if there are specific molecular changes

corresponding to a particular transport parameter. For instance, is there reduced anterograde velocity because there are less kinesin motors attached, or because there are less MIRO proteins forming the adaptor complex, or because there are more dynein motors attached, or is the reduced velocity due to something else? Therefore, quantifying the protein amounts of the transport machinery in adult S81L flies would help determine the mechanism by which mitochondrial transport is reduced. Other future directions could include analyzing other parameters of mitochondrial transport such as number of pauses and oscillations. These, combined with run length and duty cycle, can give a more complete picture of mitochondrial movement.

Another potential future direction would be to investigate the rates of anterograde vs retrograde transport in the larval system. As mentioned, there were more mitochondria moving in the anterograde direction compared to the retrograde direction, likely to aid in neuronal development. This then raises the question of mitochondrial accumulation in distal sites. The accumulation of mitochondria at neuromuscular junctions and synapses is normal as they aid in neurotransmission, however, abnormal accumulation can occur (Plucińska and Misgeld, 2016; Shidara and Hollenbeck, 2010). A recent study demonstrated local mitophagy initiates in synapses, and mitochondria are subsequently transported in the retrograde direction to minimize abnormal mitochondrial accumulation in synapses (Han et al., 2020). While this study used an AD mouse model, it could suggest a mechanism also exists in developing larvae to prevent mitochondrial accumulation. Thus, a future direction investigating a potential unknown mechanism to prevent mitochondrial accumulation could help further elucidate the rates of anterograde

and retrograde transport in this larval model system. A final future direction would be to intentionally photobleach a segment of the larval axon for better mitochondrial movement visualization. Larval motor nerves contain axon bundles, thus there are many axons with mitochondria within an imaged confocal plane. This leads to mitochondria disappearing behind other axons and/or stationary mitochondria during imaging. For example, in the present study only mitochondria that were visible for 60 consecutive frames were imaged. There were several times where a mitochondrion was visible for just over 60 frames and then disappeared. This led to these mitochondria displaying short distances, when in reality, they likely traveled much further than that. Therefore, photobleaching a small segment of the larval motor neuron would allow much better visualization of motile mitochondria, and thus could provide more accurate data.

Something else to consider is sample size and statistical power. Five males and five females were used for each genotype for a sample size of five per group. Using a sample size calculator, it was determined that a sample size around 18 per sex would yield an 80% chance of correctly rejecting the null hypothesis (Power = 0.80). Thus, for flux and percentage of mitochondrial movement, the present study was underpowered. This, paired with large variations and standard deviations, may be a potential reason why some data that looked like it would be statistically significant, was in fact not. For example, 1x S81L male mitochondria had significantly lower anterograde flux rates compared to the control (Figure 7 D). Based on bar height, it would appear that double homozygous WT male mitochondria would also produce a statistically significant difference in anterograde flux compared to the control since the difference in bar height

appears similar to the difference in bar height between 1x S81L and the control (Figure 7 F, D). However, double homozygous WT expression did not produce a statistically significant result. This could be due to the large standard deviation present in the double homozygous WT group that was not present in the 1x S81L group.

Furthermore, there were several instances where the absolute effect size (AES) between the control and experimental group were theoretically large enough to produce statistical significance, but the p-value was greater than 0.05. For instance, 1x WT expression in males resulted in a p-value of 0.0791 and an AES of 1.40 for anterograde flux. 1x S81L expression in females resulted in an AES of 1.54 and a p-value of 0.1504 for anterograde flux. While the p-value is not small, the AES was larger than it was for 1x WT males, even though 1x WT expression in males produced a smaller p-value. This indicates that the effect size may have been large enough to produce a statistically significant result, however, likely due to the large standard deviation present in the control, it resulted in statistically nonsignificant data (Type II error) (Figure 8 D). This possible Type II error is also present in male double homozygous WT mitochondria and female double homozygous S81L mitochondria for anterograde flux. As mentioned, double homozygous WT expression in males did not result in a statistically significant difference for anterograde flux ($p = 0.239$), likely due to its large standard deviation. However, the AES was 1.60 which is even higher than the AES for male 1x WT expression (1.40, $p = 0.0791$), suggesting that male double homozygous WT could have theoretically produced statistically significant results for anterograde flux if it were not for its large standard deviation (Figure 7 F). Similar to double homozygous WT males,

double homozygous S81L females had an AES of 1.60 ($p = 0.265$), but a large standard deviation, and therefore is likely a reason that despite having an appropriate AES, double homozygous S81L expression in females did not produce a statistically significant difference for anterograde flux (Figure 8 F). This large effect size that theoretically could produce statistical significance if it were not for large standard deviations is also present in 1x S81L female mitochondria for retrograde velocity (Figure 12 D), 2x S81L male mitochondria for anterograde velocity (Figure 11 E), 2x S81L female mitochondria for retrograde velocity and distance (Figure 12 E; Figure 14 E), double homozygous S81L male mitochondria for the percentage of time retrograde mitochondria spent moving in the anterograde and retrograde directions (Figure 17 F), and double homozygous S81L female mitochondria for anterograde velocity (Figure 12 C), the percentage of time anterograde mitochondria spent moving in the anterograde direction (Figure 18 C), and the percentage of time retrograde mitochondria spent moving in the retrograde direction (Figure 18 F). While increasing the sample size may or may not have an impact on the spread of the data, increasing the sample size will increase the confidence of the accuracy of the data. Therefore, increasing the sample size for future experiments may help address Type II errors, as well as to build confidence in the accuracy of the data.

One limitation was the timing of the entire study. When this project initially started, only the heterozygous model was utilized. As this was at the beginning of the study, the larval dissection method had not been perfected. When the homozygous model was introduced, it was months after the heterozygous dissections, and therefore the method had been developed more. Then because the data between the heterozygous

model and homozygous models were inconsistent, a double homozygous model was introduced a few months after the homozygous model was utilized. This double homozygous model was the model used in cell biological and behavioral studies to determine motor neuron-derived phenotypes in our previous study done by Baek et al. (2021). However, our most recently acquired data using the same double homozygous model that showed morphological neuromuscular junction defects and behavioral abnormalities observed in Baek's study suggests that mitochondrial transport defects were not a significant contributor for the abnormal morphological and behavioral phenotypes. Overall, all the data collection for the present study took place over almost 2 years during which the skill for the dissections greatly improved. While the tracking analysis remained consistent throughout the study, the sample preparation, which is often one of the most important parts of obtaining accurate data, drastically differed from the beginning to the end of this study, and thus could have an impact on the interpretation of the current data.

In summary, the ALS-FTD-causing mutation CHCHD10^{S59L} did lead to abnormal mitochondrial transport in motor neurons, but overall, there was no widespread reduction in mitochondrial motility as expected, although I observed statistically significant reductions of flux, distance, and run length of anterograde mitochondria in heterozygous male S81L larvae. The lack of widespread reduction in motility could be explained by the larval model system used, as larvae likely have a greater need for mitochondrial motility to aid in their development. Repeating this project in the adult fruit fly system would help determine if the CHCHD10^{S59L} mutation really does lead to abnormal mitochondrial

transport, and more specifically, reduced mitochondrial transport in motor neurons. This combined with other future directions such as utilizing an *in vitro* model would help to further elucidate the role, if any, that mitochondrial transport has on the pathogenesis of CHCHD10^{S59L}-mediated ALS-FTD.

References

Abramzon, Y.A., Fratta, P., Traynor, B.J., Chia, R., 2020. The Overlapping Genetics of Amyotrophic Lateral Sclerosis and Frontotemporal Dementia. Front. Neurosci. 14.

Adán, C., Matsushima, Y., Hernández-Sierra, R., Marco-Ferreres, R., Fernández-Moreno, M.Á., González-Vioque, E., Calleja, M., Aragón, J.J., Kaguni, L.S., Garesse, R., 2008. Mitochondrial Transcription Factor B2 Is Essential for Metabolic Function in Drosophila melanogaster Development *. J. Biol. Chem. 283, 12333–12342. https://doi.org/10.1074/jbc.M801342200

Ajroud-Driss, S., Fecto, F., Ajroud, K., Lalani, I., Calvo, S.E., Mootha, V.K., Deng, H.-X., Siddique, N., Tahmoush, A.J., Heiman-Patterson, T.D., Siddique, T., 2015. Mutation in the novel nuclear-encoded mitochondrial protein CHCHD10 in a family with autosomal dominant mitochondrial myopathy. neurogenetics 16, 1–9. https://doi.org/10.1007/s10048-014-0421-1

Akçimen, F., Lopez, E.R., Landers, J.E., Nath, A., Chiò, A., Chia, R., Traynor, B.J., 2023. Amyotrophic lateral sclerosis: translating genetic discoveries into therapies. Nat. Rev. Genet. 24, 642–658. https://doi.org/10.1038/s41576-023-00592-y

Al-Chalabi, A., Calvo, A., Chio, A., Colville, S., Ellis, C.M., Hardiman, O., Heverin, M., Howard, R.S., Huisman, M.H.B., Keren, N., Leigh, P.N., Mazzini, L., Mora, G., Orrell, R.W., Rooney, J., Scott, K.M., Scotton, W.J., Seelen, M., Shaw, C.E., Sidle, K.S., Swingler, R., Tsuda, M., Veldink, J.H., Visser, A.E., Berg, L.H. van den, Pearce, N., 2014. Analysis of amyotrophic lateral sclerosis as a multistep process: a population-based modelling study. Lancet Neurol. 13, 1108–1113. https://doi.org/10.1016/S1474-4422(14)70219-4

Alnaes, E., Rahamimoff, R., 1975. On the role of mitochondria in transmitter release from motor nerve terminals. J. Physiol. 248, 285–306. https://doi.org/10.1113/jphysiol.1975.sp010974

Amyotrophic lateral sclerosis (ALS) - Symptoms and causes [WWW Document], n.d. . Mayo Clin. URL https://www.mayoclinic.org/diseases-conditions/amyotrophic-lateral-sclerosis/symptoms-causes/syc-20354022 (accessed 7.22.24).

Anderson, C.J., Bredvik, K., Burstein, S.R., Davis, C., Meadows, S.M., Dash, J., Case, L., Milner, T.A., Kawamata, H., Zuberi, A., Piersigilli, A., Lutz, C., Manfredi, G., 2019. ALS/FTD mutant CHCHD10 mice reveal a tissue-specific toxic gain-of-function and mitochondrial stress response. Acta Neuropathol. (Berl.) 138, 103–121. https://doi.org/10.1007/s00401-019-01989-y

Baek, M., Choe, Y.-J., Bannwarth, S., Kim, J., Maitra, S., Dorn, G.W., Taylor, J.P., Paquis-Flucklinger, V., Kim, N.C., 2021. TDP-43 and PINK1 mediate CHCHD10 S59L mutation–induced defects in Drosophila and in vitro. Nat. Commun. 12, 1924. https://doi.org/10.1038/s41467-021-22145-9

Bannwarth, S., Ait-El-Mkadem, S., Chaussenot, A., Genin, E.C., Lacas-Gervais, S., Fragaki, K., Berg-Alonso, L., Kageyama, Y., Serre, V., Moore, D.G., Verschueren, A., Rouzier, C., Le Ber, I., Augé, G., Cochaud, C., Lespinasse, F., N'Guyen, K., de Septenville, A., Brice, A., Yu-Wai-Man, P., Sesaki, H., Pouget, J., Paquis-Flucklinger, V., 2014. A mitochondrial origin for frontotemporal dementia and

amyotrophic lateral sclerosis through CHCHD10 involvement. Brain 137, 2329–2345. https://doi.org/10.1093/brain/awu138
Barnhart, E.L., 2016. Mechanics of mitochondrial motility in neurons. Curr. Opin. Cell Biol., Cell architecture 38, 90–99. https://doi.org/10.1016/j.ceb.2016.02.022
Beal, M.F., 2005. Mitochondria take center stage in aging and neurodegeneration. Ann. Neurol. 58, 495–505. https://doi.org/10.1002/ana.20624
Beal, M.F., 1998. Mitochondrial dysfunction in neurodegenerative diseases. Biochim. Biophys. Acta BBA - Bioenerg. 1366, 211–223. https://doi.org/10.1016/S0005-2728(98)00114-5
Bernstein, B.W., Bamburg, J.R., 2003. Actin-ATP hydrolysis is a major energy drain for neurons. J. Neurosci. Off. J. Soc. Neurosci. 23, 1–6. https://doi.org/10.1523/JNEUROSCI.23-01-00002.2003
Boillée, S., Vande Velde, C., Cleveland, D.W., 2006. ALS: A Disease of Motor Neurons and Their Nonneuronal Neighbors. Neuron 52, 39–59. https://doi.org/10.1016/j.neuron.2006.09.018
Cai, Q., Sheng, Z.-H., 2009. Mitochondrial transport and docking in axons. Exp. Neurol., Mitochondria and Neurodegeneration 218, 257–267. https://doi.org/10.1016/j.expneurol.2009.03.024
Calkins, M.J., Manczak, M., Mao, P., Shirendeb, U., Reddy, P.H., 2011. Impaired mitochondrial biogenesis, defective axonal transport of mitochondria, abnormal mitochondrial dynamics and synaptic degeneration in a mouse model of Alzheimer's disease. Hum. Mol. Genet. 20, 4515–4529. https://doi.org/10.1093/hmg/ddr381
Canty, J.T., Hensley, A., Aslan, M., Jack, A., Yildiz, A., 2023. TRAK adaptors regulate the recruitment and activation of dynein and kinesin in mitochondrial transport. Nat. Commun. 14, 1376. https://doi.org/10.1038/s41467-023-36945-8
Chang, D.T.W., Reynolds, I.J., 2006. Mitochondrial trafficking and morphology in healthy and injured neurons. Prog. Neurobiol. 80, 241–268. https://doi.org/10.1016/j.pneurobio.2006.09.003
Chen, Y., Sheng, Z.-H., 2013. Kinesin-1–syntaphilin coupling mediates activity-dependent regulation of axonal mitochondrial transport. J. Cell Biol. 202, 351–364. https://doi.org/10.1083/jcb.201302040
Chistiakov, D.A., Shkurat, T.P., Melnichenko, A.A., Grechko, A.V., Orekhov, A.N., 2018. The role of mitochondrial dysfunction in cardiovascular disease: a brief review. Ann. Med. 50, 121–127. https://doi.org/10.1080/07853890.2017.1417631
Ciubuc-Batcu, M.T., Stapelberg, N.J.C., Headrick, J.P., Renshaw, G.M.C., 2024. A mitochondrial nexus in major depressive disorder: Integration with the psycho-immune-neuroendocrine network. Biochim. Biophys. Acta BBA - Mol. Basis Dis. 1870, 166920. https://doi.org/10.1016/j.bbadis.2023.166920
Corcia, P., Couratier, P., Blasco, H., Andres, C.R., Beltran, S., Meininger, V., Vourc'h, P., 2017. Genetics of amyotrophic lateral sclerosis. Rev. Neurol. (Paris), Motor neuron diseases 173, 254–262. https://doi.org/10.1016/j.neurol.2017.03.030
Course, M.M., Wang, X., 2016. Transporting mitochondria in neurons. F1000Research 5, F1000 Faculty Rev-1735. https://doi.org/10.12688/f1000research.7864.1

Dadon-Nachum, M., Melamed, E., Offen, D., 2011. The “Dying-Back” Phenomenon of Motor Neurons in ALS. J. Mol. Neurosci. 43, 470–477. https://doi.org/10.1007/s12031-010-9467-1

de Medeiros, L.M., De Bastiani, M.A., Rico, E.P., Schonhofen, P., Pfaffenseller, B., Wollenhaupt-Aguiar, B., Grun, L., Barbé-Tuana, F., Zimmer, E.R., Castro, M.A.A., Parsons, R.B., Klamt, F., 2019. Cholinergic Differentiation of Human Neuroblastoma SH-SY5Y Cell Line and Its Potential Use as an In vitro Model for Alzheimer’s Disease Studies. Mol. Neurobiol. 56, 7355–7367. https://doi.org/10.1007/s12035-019-1605-3

De Vos, K.J., Chapman, A.L., Tennant, M.E., Manser, C., Tudor, E.L., Lau, K.-F., Brownlees, J., Ackerley, S., Shaw, P.J., McLoughlin, D.M., Shaw, C.E., Leigh, P.N., Miller, C.C.J., Grierson, A.J., 2007. Familial amyotrophic lateral sclerosis-linked SOD1 mutants perturb fast axonal transport to reduce axonal mitochondria content. Hum. Mol. Genet. 16, 2720–2728. https://doi.org/10.1093/hmg/ddm226

Devine, M.J., Kittler, J.T., 2018. Mitochondria at the neuronal presynapse in health and disease. Nat. Rev. Neurosci. 19, 63–80. https://doi.org/10.1038/nrn.2017.170

Devireddy, S., Sung, H., Liao, P.-C., Garland-Kuntz, E., Hollenbeck, P.J., 2014. Chapter Eight - Analysis of Mitochondrial Traffic in Drosophila, in: Murphy, A.N., Chan, D.C. (Eds.), Methods in Enzymology, Mitochondrial Function. Academic Press, pp. 131–150. https://doi.org/10.1016/B978-0-12-801415-8.00008-4

Dorn, G.W., 2021. Mitofusin activation enhances mitochondrial motility and promotes neuroregeneration in CMT2A. Neural Regen. Res. 16, 2201–2203. https://doi.org/10.4103/1673-5374.310684

Encinas, M., Iglesias, M., Liu, Y., Wang, H., Muhaisen, A., Ceña, V., Gallego, C., Comella, J.X., 2000. Sequential Treatment of SH-SY5Y Cells with Retinoic Acid and Brain-Derived Neurotrophic Factor Gives Rise to Fully Differentiated, Neurotrophic Factor-Dependent, Human Neuron-Like Cells. J. Neurochem. 75, 991–1003. https://doi.org/10.1046/j.1471-4159.2000.0750991.x

Fischer, F., Hamann, A., Osiewacz, H.D., 2012. Mitochondrial quality control: an integrated network of pathways. Trends Biochem. Sci. 37, 284–292. https://doi.org/10.1016/j.tibs.2012.02.004

Flannery, P.J., Trushina, E., 2019. Mitochondrial dynamics and transport in Alzheimer’s disease. Mol. Cell. Neurosci. 98, 109–120. https://doi.org/10.1016/j.mcn.2019.06.009

Frederick, R.L., Shaw, J.M., 2007. Moving Mitochondria: Establishing Distribution of an Essential Organelle. Traffic 8, 1668–1675. https://doi.org/10.1111/j.1600-0854.2007.00644.x

Galvin, J.E., Howard, D.H., Denny, S.S., Dickinson, S., Tatton, N., 2017. The social and economic burden of frontotemporal degeneration. Neurology 89, 2049–2056. https://doi.org/10.1212/WNL.0000000000004614

Ghasemi, M., Brown, R.H., 2018. Genetics of Amyotrophic Lateral Sclerosis. Cold Spring Harb. Perspect. Med. 8, a024125. https://doi.org/10.1101/cshperspect.a024125

Grad, L.I., Rouleau, G.A., Ravits, J., Cashman, N.R., 2017. Clinical Spectrum of Amyotrophic Lateral Sclerosis (ALS). Cold Spring Harb. Perspect. Med. 7, a024117. https://doi.org/10.1101/cshperspect.a024117

Granatiero, V., Manfredi, G., 2019. Mitochondrial Transport and Turnover in the Pathogenesis of Amyotrophic Lateral Sclerosis. Biology 8, 36. https://doi.org/10.3390/biology8020036

Grossman, M., Seeley, W.W., Boxer, A.L., Hillis, A.E., Knopman, D.S., Ljubenov, P.A., Miller, B., Piguet, O., Rademakers, R., Whitwell, J.L., Zetterberg, H., van Swieten, J.C., 2023. Frontotemporal lobar degeneration. Nat. Rev. Dis. Primer 9, 1–19. https://doi.org/10.1038/s41572-023-00447-0

Han, S., Jeong, Y.Y., Sheshadri, P., Su, X., Cai, Q., 2020. Mitophagy regulates integrity of mitochondria at synapses and is critical for synaptic maintenance. EMBO Rep. 21, e49801. https://doi.org/10.15252/embr.201949801

Jacobs, H.T., George, J., Kemppainen, E., 2020. Regulation of growth in Drosophila melanogaster: the roles of mitochondrial metabolism. J. Biochem. (Tokyo) 167, 267–277. https://doi.org/10.1093/jb/mvaa002

Keith, J.L., Swinkin, E., Gao, A., Alminawi, S., Zhang, M., McGoldrick, P., McKeever, P., Robertson, J., Rogaeva, E., Zinman, L., 2020. Neuropathologic description of CHCHD10 mutated amyotrophic lateral sclerosis. Neurol. Genet. 6. https://doi.org/10.1212/NXG.0000000000000394

Kim, H.J., Magranè, J., Starkov, A.A., Manfredi, G., 2012. The mitochondrial calcium regulator cyclophilin D is an essential component of oestrogen-mediated neuroprotection in amyotrophic lateral sclerosis. Brain 135, 2865–2874. https://doi.org/10.1093/brain/aws208

Li, J., Yang, D., Li, Z., Zhao, M., Wang, D., Sun, Z., Wen, P., Dai, Y., Gou, F., Ji, Y., Zhao, D., Yang, L., 2023. PINK1/Parkin-mediated mitophagy in neurodegenerative diseases. Ageing Res. Rev. 84, 101817. https://doi.org/10.1016/j.arr.2022.101817

Lin, M.-Y., Sheng, Z.-H., 2015. Regulation of mitochondrial transport in neurons. Exp. Cell Res. 334, 35–44. https://doi.org/10.1016/j.yexcr.2015.01.004

Louie, K., Russo, G.J., Salkoff, D.B., Wellington, A., Zinsmaier, K.E., 2008. Effects of imaging conditions on mitochondrial transport and length in larval motor axons of Drosophila. Comp. Biochem. Physiol. A. Mol. Integr. Physiol. 151, 159–172. https://doi.org/10.1016/j.cbpa.2008.06.023

Magrané, J., Cortez, C., Gan, W.-B., Manfredi, G., 2014. Abnormal mitochondrial transport and morphology are common pathological denominators in SOD1 and TDP43 ALS mouse models. Hum. Mol. Genet. 23, 1413–1424. https://doi.org/10.1093/hmg/ddt528

Marinkovic, P., Reuter, M.S., Brill, M.S., Godinho, L., Kerschensteiner, M., Misgeld, T., 2012. Axonal transport deficits and degeneration can evolve independently in mouse models of amyotrophic lateral sclerosis. Proc. Natl. Acad. Sci. U. S. A. 109, 4296–4301. https://doi.org/10.1073/pnas.1200658109

Mattson, M.P., Gleichmann, M., Cheng, A., 2008. Mitochondria in Neuroplasticity and Neurological Disorders. Neuron 60, 748–766. https://doi.org/10.1016/j.neuron.2008.10.010

Mejzini, R., Flynn, L.L., Pitout, I.L., Fletcher, S., Wilton, S.D., Akkari, P.A., 2019. ALS Genetics, Mechanisms, and Therapeutics: Where Are We Now? Front. Neurosci. 13, 1310. https://doi.org/10.3389/fnins.2019.01310

Millecamps, S., Julien, J.-P., 2013. Axonal transport deficits and neurodegenerative diseases. Nat. Rev. Neurosci. 14, 161–176. https://doi.org/10.1038/nrn3380

Misko, A., Jiang, S., Wegorzewska, I., Milbrandt, J., Baloh, R.H., 2010. Mitofusin 2 Is Necessary for Transport of Axonal Mitochondria and Interacts with the Miro/Milton Complex. J. Neurosci. 30, 4232–4240. https://doi.org/10.1523/JNEUROSCI.6248-09.2010

Moller, A., Bauer, C.S., Cohen, R.N., Webster, C.P., De Vos, K.J., 2017. Amyotrophic lateral sclerosis-associated mutant SOD1 inhibits anterograde axonal transport of mitochondria by reducing Miro1 levels. Hum. Mol. Genet. 26, 4668–4679. https://doi.org/10.1093/hmg/ddx348

Morris, R.L., Hollenbeck, P.J., 1993. The regulation of bidirectional mitochondrial transport is coordinated with axonal outgrowth. J. Cell Sci. 104, 917–927. https://doi.org/10.1242/jcs.104.3.917

Neisch, A.L., Avery, A.W., Machamer, J.B., Li, M., Hays, T.S., 2016. Methods to identify and analyze gene products involved in neuronal intracellular transport using *Drosophila*, in: Pfister, K.K. (Ed.), Methods in Cell Biology, The Neuronal Cytoskeleton, Motor Proteins, and Organelle Trafficking in the Axon. Academic Press, pp. 277–309. https://doi.org/10.1016/bs.mcb.2015.06.015

Nelson, L.M., Topol, B., Kaye, W., Williamson, D., Horton, D.K., Mehta, P., Wagner, T., 2018. Estimation of the Prevalence of Amyotrophic Lateral Sclerosis in the United States Using National Administrative Healthcare Data from 2002 to 2004 and Capture-Recapture Methodology. Neuroepidemiology 51, 149–157. https://doi.org/10.1159/000488798

Nguyen, H.P., Van Broeckhoven, C., van der Zee, J., 2018. ALS Genes in the Genomic Era and their Implications for FTD. Trends Genet. 34, 404–423. https://doi.org/10.1016/j.tig.2018.03.001

Ni, H.-M., Williams, J.A., Ding, W.-X., 2015. Mitochondrial dynamics and mitochondrial quality control. Redox Biol. 4, 6–13. https://doi.org/10.1016/j.redox.2014.11.006

Nunnari, J., Suomalainen, A., 2012. Mitochondria: In sickness and in health. Cell 148, 1145–1159. https://doi.org/10.1016/j.cell.2012.02.035

Plucińska, G., Misgeld, T., 2016. Imaging of neuronal mitochondria *in situ*. Curr. Opin. Neurobiol., Cellular neuroscience 39, 152–163. https://doi.org/10.1016/j.conb.2016.06.006

Rademakers, R., Hutton, M., 2007. The genetics of frontotemporal lobar degeneration. Curr. Neurol. Neurosci. Rep. 7, 434–442. https://doi.org/10.1007/s11910-007-0067-6

Radford, R.A., Morsch, M., Rayner, S.L., Cole, N.J., Pountney, D.L., Chung, R.S., 2015. The established and emerging roles of astrocytes and microglia in amyotrophic lateral sclerosis and frontotemporal dementia. Front. Cell. Neurosci. 9.

Riedl, L., Mackenzie, I.R., Förstl, H., Kurz, A., Diehl-Schmid, J., 2014. Frontotemporal lobar degeneration: current perspectives. Neuropsychiatr. Dis. Treat. 10, 297–310. https://doi.org/10.2147/NDT.S38706

Ruthel, G., Hollenbeck, P.J., 2003. Response of Mitochondrial Traffic to Axon Determination and Differential Branch Growth. J. Neurosci. 23, 8618–8624. https://doi.org/10.1523/JNEUROSCI.23-24-08618.2003

Sakagami, H., Suzuki, R., Shirataki, Y., Iwama, S., Nakagawa, M., Suzuki, H., Tanaka, K., Tamura, N., Takeshima, H., 2017. Re-evaluation of Culture Condition of PC12 and SH-SY5Y Cells Based on Growth Rate and Amino Acid Consumption. In Vivo 31, 1089–1095.

Shanmughapriya, S., Langford, D., Natarajaseenivasan, K., 2020. Inter and Intracellular mitochondrial trafficking in health and disease. Ageing Res. Rev. 62, 101128. https://doi.org/10.1016/j.arr.2020.101128

Sheng, Z.-H., Cai, Q., 2012. Mitochondrial transport in neurons: impact on synaptic homeostasis and neurodegeneration. Nat. Rev. Neurosci. 13, 77–93. https://doi.org/10.1038/nrn3156

Shi, P., Ström, A.-L., Gal, J., Zhu, H., 2010. Effects of ALS-related SOD1 mutants on dynein- and KIF5-mediated retrograde and anterograde axonal transport. Biochim. Biophys. Acta BBA - Mol. Basis Dis. 1802, 707–716. https://doi.org/10.1016/j.bbadis.2010.05.008

Shidara, Y., Hollenbeck, P.J., 2010. Defects in Mitochondrial Axonal Transport and Membrane Potential without Increased Reactive Oxygen Species Production in a Drosophila Model of Friedreich Ataxia. J. Neurosci. 30, 11369–11378. https://doi.org/10.1523/JNEUROSCI.0529-10.2010

Shipley, M.M., Mangold, C.A., Szpara, M.L., 2016. Differentiation of the SH-SY5Y Human Neuroblastoma Cell Line. JoVE J. Vis. Exp. e53193. https://doi.org/10.3791/53193

Smith, G.M., Gallo, G., 2018. The role of mitochondria in axon development and regeneration. Dev. Neurobiol. 78, 221–237. https://doi.org/10.1002/dneu.22546

Tennessen, J.M., Baker, K.D., Lam, G., Evans, J., Thummel, C.S., 2011. The Drosophila Estrogen-Related Receptor Directs a Metabolic Switch that Supports Developmental Growth. Cell Metab. 13, 139–148. https://doi.org/10.1016/j.cmet.2011.01.005

Tiwari, S.K., Mandal, S., 2021. Mitochondrial Control of Stem Cell State and Fate: Lessons From Drosophila. Front. Cell Dev. Biol. 9. https://doi.org/10.3389/fcell.2021.606639

Truman, J.W., Riddiford, L.M., 2023. Drosophila postembryonic nervous system development: a model for the endocrine control of development. Genetics 223, iyac184. https://doi.org/10.1093/genetics/iyac184

Visentin, D.C., Cleary, M., Hunt, G.E., 2020. The earnestness of being important: Reporting non-significant statistical results. J. Adv. Nurs. 76, 917–919. https://doi.org/10.1111/jan.14283

Wang, X., Schwarz, T.L., 2009. The Mechanism of Ca2+-Dependent Regulation of Kinesin-Mediated Mitochondrial Motility. Cell 136, 163–174. https://doi.org/10.1016/j.cell.2008.11.046

Wang, X., Winter, D., Ashrafi, G., Schlehe, J., Wong, Y.L., Selkoe, D., Rice, S., Steen, J., LaVoie, M.J., Schwarz, T.L., 2011. PINK1 and Parkin Target Miro for Phosphorylation and Degradation to Arrest Mitochondrial Motility. Cell 147, 893–906. https://doi.org/10.1016/j.cell.2011.10.018

Wijesekera, L.C., Nigel Leigh, P., 2009. Amyotrophic lateral sclerosis. Orphanet J. Rare Dis. 4, 3. https://doi.org/10.1186/1750-1172-4-3

Xie, Y., Zhou, B., Lin, M.-Y., Wang, S., Foust, K.D., Sheng, Z.-H., 2015. Endolysosomal Deficits Augment Mitochondria Pathology in Spinal Motor Neurons of Asymptomatic fALS Mice. Neuron 87, 355–370. https://doi.org/10.1016/j.neuron.2015.06.026

Zheng, Y.-R., Zhang, X.-N., Chen, Z., 2019. Mitochondrial transport serves as a mitochondrial quality control strategy in axons: Implications for central nervous system disorders. CNS Neurosci. Ther. 25, 876–886. https://doi.org/10.1111/cns.13122

Supplementary Information

Supplementary Figure 1: A summary heat map for mitochondrial motility in WT flies of all the parameters, taking direction into account. Red color indicates a statistically significant increase in mitochondrial motility compared to the control. Pink color indicated that parameter showed a trend for increased motility compared to the control. Blue color indicates a statistically significant decrease in mitochondrial motility compared to the control. Light blue color indicates that parameter showed a trend for decreased motility compared to the control. White boxes indicate there was no statistical significance.

Supplementary Table 1: Summary table of statistical significance for mitochondrial transport in male WT flies compared to their respective control genotype. The last row is the trend WT mitochondria exhibit compared to the control when considering statistically significant data (dark colored boxes in Supplementary Figure 1) and trends of statistically significant data (light colored boxed in Supplementary Figure 1). NS: nonsignificant. AS: net Anterograde mitochondria that are Stationary. AA: net Anterograde mitochondria move in the Anterograde direction. RS: net Retrograde mitochondria that are Stationary. RR: net Retrograde mitochondria reversing to move in the Retrograde direction.

	Heterozygous Model	**Homozygous Model**	**Double Homozygous Model**
Flux	NS	NS	NS
Percent Mitochondrial Movement	NS	NS	NS
Velocity	Faster in the anterograde direction	Faster in the anterograde direction	Slower in the anterograde direction
Distance	Shorter in the anterograde direction	NS	Shorter in the retrograde direction
Run Length	Shorter in the anterograde direction	NS	NS
Duty Cycle	NS	Less AS, more AA	More AS, less AA. More RS, less RR
Overall Movement Trend Compared to Control	Reduced	Increased	Reduced

Supplementary Table 2: Summary table of statistical significance for mitochondrial transport in female WT flies compared to their respective control genotype. The last row is the trend WT mitochondria exhibit compared to the control when considering statistically significant data (dark colored boxes in Supplementary Figure 1) and trends of statistically significant data (light colored boxed in Supplementary Figure 1). NS: nonsignificant. AS: net Anterograde mitochondria that are Stationary. AR: net Anterograde mitochondria move in the Retrograde direction.

	Heterozygous Model	**Homozygous Model**	**Double Homozygous Model**
Flux	NS	NS	NS
Percent Mitochondrial Movement	NS	NS	NS
Velocity	Faster in anterograde and retrograde directions	NS	Slower in anterograde and retrograde directions
Distance	NS	NS	NS
Run Length	Longer in anterograde and retrograde directions	NS	Shorter in the retrograde direction
Duty Cycle	NS	Less AS, more AR	NS
Overall Movement Trend Compared to Control	Increased	Increased	Reduced